The maximum rate of mammal evolution

Alistair R. Evans[a,1], David Jones[a,b], Alison G. Boyer[c], James H. Brown[d,e,1], Daniel P. Costa[f], S. K. Morgan Ernest[g], Erich M. G. Fitzgerald[h], Mikael Fortelius[i], John L. Gittleman[j], Marcus J. Hamilton[d,e,k], Larisa E. Harding[l], Kari Lintulaakso[i], S. Kathleen Lyons[m], Jordan G. Okie[d,n], Juha J. Saarinen[i], Richard M. Sibly[o], Felisa A. Smith[d], Patrick R. Stephens[j], Jessica M. Theodor[p], and Mark D. Uhen[q]

[a]School of Biological Sciences, Monash University, VIC 3800, Australia; [b]School of Earth Sciences, University of Bristol, Bristol BS8 1RJ, United Kingdom; [c]Department of Ecology and Evolutionary Biology, University of Tennessee, Knoxville, TN 37996; [d]Department of Biology, University of New Mexico, Albuquerque, NM 87131; [e]Santa Fe Institute, Santa Fe, NM 87501; [f]Department of Ecology and Evolutionary Biology, University of California, Santa Cruz, CA 95060; [g]Department of Biology and Ecology Center, Utah State University, Logan, UT 84322; [h]Geosciences, Museum Victoria, Melbourne, VIC 3001, Australia; [i]Department of Geosciences and Geography and Finnish Museum of Natural History, University of Helsinki, Helsinki, FIN-00014, Finland; [j]Odum School of Ecology, University of Georgia, Athens, GA 30602; [k]Department of Anthropology, University of New Mexico, Albuquerque, NM 87131; [l]Landscape Ecology, Department of Ecology and Environmental Science, Umeå University, SE-90187 Umeå, Sweden; [m]Smithsonian Institution, Washington, DC 20013; [n]School of Earth and Space Exploration, Arizona State University, Tempe, AZ 85287 [o]School of Biological Sciences, University of Reading, Reading RG6 6AH, United Kingdom; [p]Department of Biological Sciences, University of Calgary, Calgary, AB, Canada T2N 1N4; and [q]Department of Atmospheric, Oceanic, and Earth Sciences, George Mason University, Fairfax, VA 22030

Contributed by James Hemphill Brown, December 29, 2011 (sent for review October 1, 2011)

How fast can a mammal evolve from the size of a mouse to the size of an elephant? Achieving such a large transformation calls for major biological reorganization. Thus, the speed at which this occurs has important implications for extensive faunal changes, including adaptive radiations and recovery from mass extinctions. To quantify the pace of large-scale evolution we developed a metric, clade maximum rate, which represents the maximum evolutionary rate of a trait within a clade. We applied this metric to body mass evolution in mammals over the last 70 million years, during which multiple large evolutionary transitions occurred in oceans and on continents and islands. Our computations suggest that it took a minimum of 1.6, 5.1, and 10 million generations for terrestrial mammal mass to increase 100-, and 1,000-, and 5,000-fold, respectively. Values for whales were down to half the length (i.e., 1.1, 3, and 5 million generations), perhaps due to the reduced mechanical constraints of living in an aquatic environment. When differences in generation time are considered, we find an exponential increase in maximum mammal body mass during the 35 million years following the Cretaceous–Paleogene (K–Pg) extinction event. Our results also indicate a basic asymmetry in macroevolution: very large decreases (such as extreme insular dwarfism) can happen at more than 10 times the rate of increases. Our findings allow more rigorous comparisons of microevolutionary and macroevolutionary patterns and processes.

haldanes | biological time | scaling | pedomorphosis

Microevolution and macroevolution characterize two extremes of the evolutionary process, representing evolution below and above the species level, respectively (1, 2). Microevolution often exhibits very fast rates over short timescales (<100 generations). At a typical generation-to-generation rate, evolution by a random walk could hypothetically produce a body mass change from that of a 20-g mouse to that of a 2,000,000-g elephant in fewer than 200,000 generations (3), a relatively brief geological interval. However, such high rates are not sustained over long intervals in the fossil record. Presumably this is because diverse physical, functional, genetic, developmental, and ecological constraints restrict large-scale macroevolution. Because these constraints may operate differently depending on whether an organism is becoming larger or smaller, it is equally important to understand whether the reverse transformation, from elephant to mouse, would be easier. Our question is how quickly such intertwined constraints can be overcome when there is a selective advantage to do so: What is the maximum rate of macroevolution? To paraphrase G. Evelyn Hutchinson "How big was it and how fast did it happen?" (4).

Body mass is the most fundamental animal trait, strongly correlated with most aspects of morphology, life history, physiology, and behavior (5–7). Evolution of body mass influences and is influenced by selection on other traits and is easily characterized. Thus, changes in body size provide some of the best examples of rapid evolution (8, 9).

Evolutionary rates of morphological traits such as size are often quantified in haldanes (h) (10, 11), which measure proportional change in a feature (M_i) between two time points (i) standardized by the available variation (pooled ln SD s_p) using a timescale in number of generations (g): $h = (\ln M_2 - \ln M_1)/(s_p \times g)$.

However, most previous measurements of evolutionary rates have been made either for well-defined lineages in a stratigraphic sequence or pairs of time points where an ancestor/descendant relationship is reasonably certain (3, 11, 12). This tends to restrict comparisons to closely related groups with relatively small evolutionary changes and low rates.

To better characterize major changes in a phenotypic trait within a clade, as opposed to a single lineage, we developed the clade maximum rate (CMR) metric. The clade maximum rate is defined as the rate of change in a specified extreme value of a trait (either the minimum or the maximum) for a clade within a given time interval. Whereas this metric describes the rate at which the maximum of a trait increases, the CMR is normally slower than the maximum rate of evolution of the trait within individual lineages of the clade (Fig. 1). CMR intentionally ignores decreases in the maximum of the trait because these can happen by true evolutionary decreases or extinction of the lineages that achieved the maximum. A major advantage of the clade maximum rate is that a detailed phylogeny is not required, only the recognition of distinct clades.

Here, we investigated the clade maximum rate for maximum body mass. We used a compilation of the maximum body mass (M) for 28 mammal orders on the four largest continents (Africa, Eurasia, and North and South America) and all ocean basins for all subepochs during the last 70 million years, covering the well-documented mammal radiation following the Cretaceous–Paleogene (K–Pg) mass extinction (13). To test for generality of

Author contributions: A.R.E. designed research; A.R.E., D.J., A.G.B., J.H.B., D.P.C., S.K.M.E., E.M.G.F., M.F., J.L.G., M.J.H., L.E.H., K.L., S.K.L., J.G.O., J.J.S., R.M.S., F.A.S., P.R.S., J.M.T., and M.D.U. performed research; A.R.E., D.J., J.G.O., and R.M.S. contributed new reagents/analytic tools; A.R.E., D.J., M.J.H., J.G.O., R.M.S., and M.D.U. analyzed data; and A.R.E., D.J., A.G.B., J.H.B., D.P.C., S.K.M.E., E.M.G.F., M.F., J.L.G., M.J.H., L.E.H., K.L., S.K.L., J.G.O., J.J.S., R.M.S., F.A.S., P.R.S., J.M.T., and M.D.U. wrote the paper.

The authors declare no conflict of interest.

See Commentary on page 4027.

[1]To whom correspondence may be addressed. E-mail: arevans@fastmail.fm or jhbrown@unm.edu.

This article contains supporting information online at www.pnas.org/lookup/suppl/doi:10.1073/pnas.1120774109/-/DCSupplemental.

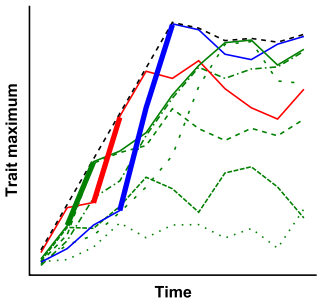

Fig. 1. Evolutionary rate of the clade maximum for a trait can underestimate the maximum evolutionary rate of subclades or component lower taxa within the clade. The black dashed line represents the maximum for a clade composed of three subclades represented by green, red, and blue lines. Each of these subclades is composed of lineages of species, shown for the green clade as thin broken lines. When a different subclade becomes the new clade maximum, it must have a higher evolutionary rate than the clade maximum for that interval: the thick lines represent this process.

the patterns, we also obtained and analyzed data for North American Artiodactyla at the finer temporal resolution of the North American Land Mammal Age (NALMA) subages. For each clade, we calculated the CMR of body size evolution in haldanes. We supplemented CMR with a reference database from the literature of 1,453 rates of mammalian body mass evolution for many phylogenetic groups at various temporal scales. A third dataset from empirical selection experiments on mouse body size (3, 14) measured evolutionary change over 1–23 generations. Directly comparing rates at different interval lengths is complicated; although a very high rate can be sustained for a short interval, over longer periods, rates tend to vary and the direction of evolution may change (12). Thus, interval length must be incorporated into any analysis.

Generation time is considered the fundamental unit of evolutionary time because evolutionary change cannot happen more quickly than a single generation (10, 11). The use of generation time rather than chronological time is crucial for the calculation of interval length because generation time increases allometrically with mass (i.e., larger species have longer generation times than smaller species). Therefore, evolutionary rates appear to slow in chronological time as the maximum size increases even when they are the same rate in generational time. If generation time were invariant with body mass, then the slope of body mass as a function of chronological time (t) would indicate a true evolutionary rate (Fig. 2*A*). However, generation time, like many other biological processes such as lifespan, gestation, lactation, and sleep cycle, scales as ~1/4 power of body mass ($M^{0.259}$) for placental mammals (*Materials and Methods*). Thus, plotting $M^{0.259}$ against time gives a generation time-corrected evolutionary rate in haldanes (Fig. 2*B*). A straight line relationship here indicates an exponential increase in maximum size over biological time (*SI Appendix*).

Results

We find that the maximum body mass of terrestrial mammals evolved at a near-constant rate from 70 million years ago (Ma), just before the K–Pg, until the appearance of the largest terrestrial mammal, *Indricotherium*, at about 30 Ma. A linear regression gives an excellent fit to this time interval, with a slope equivalent to 7.1×10^{-6} haldanes ($R^2 = 0.97$; Table 1 and Fig. 2). A similar constancy, but with somewhat different absolute rates, appears in several orders: Cetacea (from Oligocene to Recent), Artiodactyla, Perissodactyla, Proboscidea, and Rodentia, and to a lesser extent the Carnivora and Primates (Table 1). The relative constancy of evolutionary rate for maximum body mass for the 35 million years following the extinction of the nonavian dinosaurs is striking and unexpected. Our results offer a different perspective from a recent analysis of body mass evolution over chronological time, but are consistent with convergence toward an asymptote for maximum body mass globally and within each continent (13) (Fig. 2*A*).

Across all analyzed datasets, we find that the largest changes occur in the clade maximum data (Fig. 3*A*). The highest magnitudes of change are about 5,000-fold (blue, Fig. 3*A*), much greater than the 100-fold increases seen in the reference database (yellow, Fig. 3*A*). This difference occurs despite the considerable overlap between our dataset and the reference data in the time intervals studied. Using the clade maximum rates for all mammals, we estimate the minimum times to evolve 100-, 1,000-, and 5,000-fold increases in body size are 1.1, 3, and 5 million generations, respectively (Table 2) and occur in

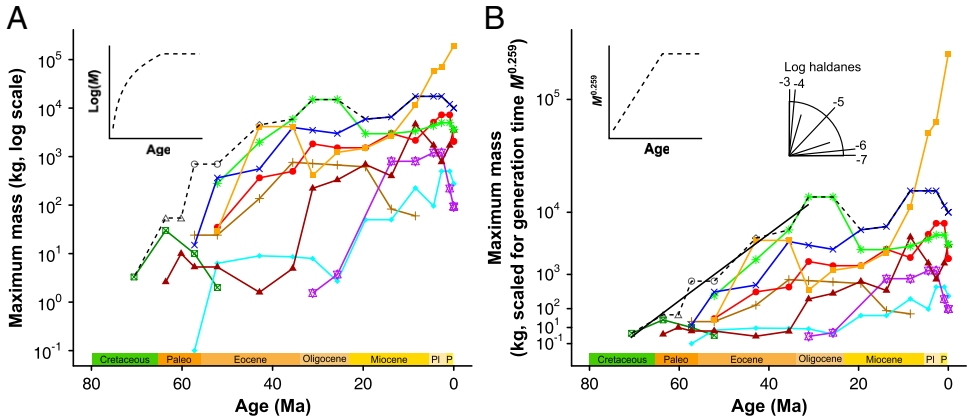

Fig. 2. Maximum mammalian body mass over time for terrestrial mammals (dashed black line) and separate mammal orders (colored lines). (*A*) Log(M) vs. Age shows an asymptotic relationship for the mammalian maximum. (*B*) Mass is scaled to the power of 0.259 on the y axis (given an empirical $M^{0.259}$ scaling of generation times), so the slope of lines indicates generation time-corrected evolutionary rates as indicated by an angular scale (haldanometer). *Inset* graphs show how an asymptotic relationship for M vs. Age can result in a linear trajectory for $M^{0.259}$ vs. Age, as found for terrestrial mammals from 70 to 30 Ma (solid black line in *B*). Rates were calculated separately for the orders in color; when other orders comprise the maximum size across all mammals, they are shown in gray. Artiodactyls (red circle), carnivorans (red triangle), cetaceans (orange square), creodonts (brown plus sign), multituberculates (green cross in square), perissodactyls (green asterisk), primates (cyan diamond), proboscideans (blue X), rodents (purple star), condylarths (open gray triangle), dinoceratans (open gray diamond), pantodonts (open gray circle). Time units: Paleo, Paleocene; Pl, Pliocene; P, Pleistocene.

Table 1. The maximum body mass for all terrestrial mammals and for several orders increased linearly when generation time is accounted for

	Slope	Haldanes ($\times 10^{-6}$)	R^2	P
Terrestrial maximum	1.59	7.14	0.97	1.17×10^{-5}
Artiodactyla	0.74	3.34	0.90	3.33×10^{-5}
Carnivora	0.65	2.94	0.74	6.87×10^{-4}
Cetacea	3.25	14.60	0.83	1.70×10^{-3}
Perissodactyla	2.13	9.57	0.98	9.70×10^{-3}
Primates	0.39	1.77	0.78	1.46×10^{-4}
Proboscidea	1.08	4.84	0.91	6.25×10^{-5}
Rodentia	1.21	5.45	0.93	1.74×10^{-3}

Slope for linear regression of $M^{0.259}$ vs. Age (Ma) for each group from their origin until their maximum (except for Cetacea, which is for the period of 31 Ma to the Recent). The average rate in haldanes was calculated using the mammalian scaling relationship of generation time with body mass (*SI Appendix*). These time intervals are plotted as points in Fig. 3*B*.

cetaceans. In contrast, the maximum evolutionary rates for terrestrial mammals are much lower, taking 1.6, 5.1, and 10 million generations, respectively (Table 2).

Discussion

Although the global data provide an overall estimate of evolutionary rates across all mammals, there is interesting and likely important variation among the clades and modes of life. The maximum body mass of cetaceans yields the highest long-term rates of any order (Table 1) and higher rates than other mammals (Fig. 3*B*). This finding may reflect the fewer mechanical constraints on body form and function in the aquatic environment (7). Moreover, a large mass is advantageous for maintaining thermoregulatory balance, so selection pressures for large size may be stronger in an aquatic environment. However, no group yielded macroevolutionary rates approaching those reported from microevolutionary studies.

The discrepancy between microevolutionary predictions for large-scale body size evolution and actual macroevolutionary measurements of rates has long been known (3, 12, 15, 16) but little understood. Although our study cannot definitively address this issue, it does furnish some important insights. We provide strong empirical evidence that the maximum rate of body size evolution decreases with increasing time interval (12, 17). Indeed, we find an approximate linear relationship across the different datasets between the maximum amount of change and the time interval: the maximum log change scales with log time interval with a slope of 0.25 (*SI Appendix*). Using this scaling relationship, we estimate that the 100,000-fold transformation from mouse to elephant would take 24 million generations. This is substantially longer than 200,000–2 million generations suggested by microevolutionary rates (3, 15).

To investigate the converse transformation of elephant to mouse, we divided our reference data into size increases and decreases. Whereas changes in mass below twofold appear to have similar maximum rates for increases and decreases in size, above this the rates are unequal (Fig. 3*B*). The largest decreases, such as insular dwarfism, are more than 30 times the rate of increases of the same magnitude (Table 2). This apparent asymmetry is especially surprising given the ample evidence for Cope's rule, a trend for body size to increase consistently and relatively continuously throughout the history of a lineage (18, 19).

The asymmetry between rates can potentially be explained by distinct but not necessarily mutually exclusive mechanisms. One possibility is that there are fewer physical, biological, and environmental constraints to decreasing as opposed to increasing size. Pedomorphic processes are good candidates as mechanisms of size reduction, because all animals must pass through a smaller size during their ontogeny. We hypothesize it is easier to halt the developmental program and reproduce early than to grow larger and delay maturity. Another possibility is that selection favors size decreases because smaller animals have higher rates of reproduction with life histories characterized by rapid maturity, high

Table 2. Minimum number of generations (millions) required to evolve various magnitudes of change in mammals

		Magnitude of change				
		×3	×10	×100	×1,000	×5,000
All mammals	Increase	0.016	0.30	1.1	3.0	5.0
Terrestrial mammals	Increase	0.016	0.30	1.6	5.1	10.0
Cetaceans	Increase	0.10	0.40	1.1	3.0	5.0
Insular dwarfism	Decrease	0.001	0.008	0.12		

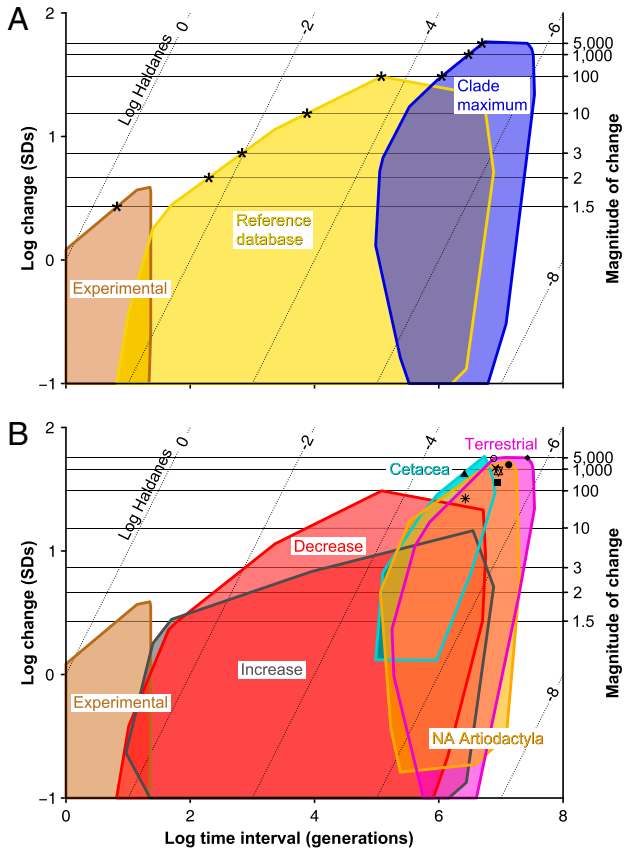

Fig. 3. Maximum rates of evolution for large changes in mammalian body mass. Minimum convex polygons of rates plotted as log change in body mass (in units of SD) vs. log time interval (generations). (*A*) The three datasets compared in this study: experimental rates (3, 14) (brown), 1,453 rates from previous studies (yellow), and clade maximum rates (blue). Asterisks indicate minimum number of generations to evolve a given amount of change. (*B*) Datasets split into components. Compiled rates are separated into increases (gray) and decreases (red) and clade maximum rates (all of which are increases) into terrestrial orders (pink), cetaceans (cyan), and North American artiodactyls (orange). Points show average rates for linear increase in Table 1 for terrestrial mammals (open circle), artiodactyls (closed circle), carnivorans (square), cetaceans (triangle), perissodactyls (asterisk), primates (diamond), proboscideans (X), and rodents (star). Right-hand *y* axis and horizontal lines illustrate magnitude of change in body mass. Large decreases (>2-fold) require substantially less time than increases, and maximum rates for very large changes (>100-fold) in cetaceans are about twice those in terrestrial. Diagonal dotted lines are isohaldanes, equal rates measured in log haldanes.

birth rates, and short lifespans (20). Finally, decreases in size may reflect adaptation to a more generalized ecological niche, whereas increases in size require novel adaptations to obtain more food and space to fuel higher whole-organism metabolic rates.

In the reference dataset, the largest decreases in body size were rates of dwarfing in large mammals after isolation on islands by rising sea levels during the last few million years: elephants on the Mediterranean islands of Sicily, Malta, and Cyprus (9, 21); mammoths on the California Channel Islands (22); and red deer on Jersey (8) (*SI Appendix*). These island dwarfism cases involve body mass changes of 5- to 100-fold over estimated time intervals of 0.006–0.8 myr or 2,300–120,000 generations. Islands characteristically have fewer predators, competitors, and resources (23), thereby favoring faster life histories and more generalized ecologies and perhaps also leading to higher selection pressures (17).

Our study represents a comprehensive analysis of large-scale macroevolutionary rates for a single trait. Whereas previous work used metrics similar to our clade maximum rates (10, 24, 25) using only two data points, our clade maximum rate metric allows assessment of rates over a range of time intervals and with high temporal resolution. This allows us to make direct quantitative comparisons of microevolutionary and macroevolutionary rates (1, 3, 12, 15, 26). Maximum macroevolutionary rates have important implications for large-scale faunal changes and recovery from mass extinction (13, 19). Our results highlight the comparative difficulty of major changes in body size, especially increasing in size. At least 5 million generations were required for a mammal to increase 1,000-fold in body mass, from the size of a rabbit to the size of an elephant. Compared with an equivalent change at microevolutionary rates, this substantial length of time illustrates just how challenging this great transformation is.

Materials and Methods

We used the compilation (13) of the maximum body mass for each of 28 orders of Mammalia in each subepoch since 70 Ma (Mammoth database v. 1.0). We calculated rates for the mammal maximum and for the nine best sampled orders using the CMR method. The maximum mass of artiodactyls in North America was calculated for 18 families for each North American Land Mammal subage. Natural log body mass SD was estimated to be 0.15 from modern species (27) as used previously (3) (*SI Appendix*). Generation time was estimated as age at first parturition. Regression equations for body mass vs. generation time calculated from the data for 839 placental mammal species and for 82 marsupial species (28) were used to estimate generation time for extinct taxa on the basis of body size. For each sequence of maxima, all combinations of time points were compared. Only rates of increase in maximum size were calculated for the maximum mammalian body size, as these must be due to evolutionary change. The pattern of increase in maximum body mass of terrestrial mammals ($M^{0.259}$) from 70 to 30 Ma was assessed with ordinary least squares (OLS), segmented, Gompertz, square root, exponential, and logistic regressions. The OLS regression model was the best fit according to Akaike information criterion (AIC) (*SI Appendix*). The pattern of increase in maximum size for seven orders was also assessed using OLS regression (Table 1). We calculated evolutionary rates for mammal data in references (3, 17, 29) where sufficient data were present in the original paper to allow estimation of body mass and time intervals. *SI Appendix* lists the sources of data for body size, generation time, and interval length for the studies used. Data quality for these sources will be variable, depending on factors such as the accuracy of the identification of ancestor-descendant pairs and the date at which the derived morphology was actually attained. Several sensitivity tests were conducted to examine whether the incompleteness of the fossil record and/or binning data by subepoch biased rate calculations. These tests comprised sets of 100 independent random walks in 10 clades for 1,000 steps in 10 intervals. The maximum within each subclade and for the whole clade was calculated for each interval. The rates of change in the subclade and clade maxima were calculated per interval as for the CMR method. Fossilization was simulated by downsampling the data to between 1 and 0.005%. Maxima in each interval and rates of change were then calculated for each subclade and clade. These calculations indicated that the estimated evolutionary rates are not significantly biased due to these effects, although at very low preservation levels variation in measured rates increased.

ACKNOWLEDGMENTS. We thank G. Evans, M. Burd, D. Dowling, Evolutionary Biology at Monash, P. Smits, G. Sanson, J. Jernvall, F. Whiteman, M. Balk, B. Van Valkenburgh, J. Damuth, A. Lister, and P. D. Polly for discussions and comments on earlier manuscripts. This study was supported by an Australian Research Council Australian Research Fellowship (to A.R.E.), Monash University Monash Research Fellowship (to A.R.E.), National Science Foundation Grant Integrating Macroecological Pattern and Processes across Scales Research Coordination Network (IMPPS RCN) DEB 0541625 (to F.A.S., S.K.L., and S.K.M.E., principal investigators), European Union Marie Curie Grant PIOF-GA-2009-235868 (to D.J.), and a Harold Mitchell Foundation Harold Mitchell Fellowship (to E.M.G.F.). This paper is IMPPS RCN publication no. 18.

1. Simpson GG (1953) *The Major Features of Evolution* (Simon and Schuster, New York).
2. Stanley SM (1979) *Macroevolution: Pattern and Process* (W. H. Freeman, San Francisco).
3. Gingerich PD (2001) Rates of evolution on the time scale of the evolutionary process. *Genetica* 112-113:127–144.
4. Hutchinson GE (1975) Variations on a theme by Robert MacArthur. *Ecology and Evolution of Communities*, eds Cody ML, Diamond JM (Belknap Press, Cambridge), pp 492–512.
5. Peters RH (1983) *The Ecological Implications of Body Size* (Cambridge Univ Press, Cambridge).
6. Calder WA (1984) *Size, Function, and Life History* (Harvard Univ Press, Cambridge, MA).
7. Schmidt-Nielsen K (1984) *Scaling: Why Is Animal Size So Important?* (Cambridge Univ Press, Cambridge).
8. Lister AM (1989) Rapid dwarfing of red deer on Jersey in the last interglacial. *Nature* 342:539–542.
9. Roth VL (1992) Inferences from allometry and fossils: Dwarfing of elephants on islands. *Oxf Surv Evol Biol* 8:259–288.
10. Haldane JBS (1949) Suggestions as to quantitative measurement of rates of evolution. *Evolution* 3:51–56.
11. Gingerich PD (1993) Quantification and comparison of evolutionary rates. *Am J Sci* 293A:453–478.
12. Gingerich PD (1983) Rates of evolution: Effects of time and temporal scaling. *Science* 22:159–161.
13. Smith FA, et al. (2010) The evolution of maximum body size of terrestrial mammals. *Science* 330:1216–1219.
14. Falconer DS (1973) Replicated selection for body weight in mice. *Genet Res* 22: 291–321.
15. Polly PD (2001) Paleontology and the comparative method: Ancestral node reconstructions versus observed node values. *Am Nat* 157:596–609.
16. Kinnison MT, Hendry AP (2001) The pace of modern life II: From rates of contemporary microevolution to pattern and process. *Genetica* 112-113:145–164.
17. Millien V (2006) Morphological evolution is accelerated among island mammals. *PLoS Biol* 4:e321.
18. Stanley SM (1973) An explanation for Cope's rule. *Evolution* 27:1–26.
19. Alroy J (1998) Cope's rule and the dynamics of body mass evolution in North American fossil mammals. *Science* 280:731–734.
20. Sibly RM, Brown JH (2007) Effects of body size and lifestyle on evolution of mammal life histories. *Proc Natl Acad Sci USA* 104:17707–17712.
21. Davies P, Lister AM (2001) *Palaeoloxodon cypriotes*, the dwarf elephant of Cyprus: Size and scaling comparisons with *P. falconeri* (Sicily-Malta) and mainland *P. antiquus*. *The World of Elephants: Proceedings of the 1st International Congress, Rome 2001*, ed Cavarretta G (Ufficio Pubblicazioni, Rome), pp 479–480.
22. Lister A, Bahn PG (2007) *Mammoths: Giants of the Ice Age* (Univ of California Press, Berkeley), Rev. Ed.
23. Lomolino MV (2005) Body size evolution in insular vertebrates: Generality of the island rule. *J Biogeogr* 32:1683–1699.
24. Colbert EH (1948) Evolution of the horned dinosaurs. *Evolution* 2:145–163.
25. Stanley SM (1985) Rates of evolution. *Paleobiology* 11:13–26.
26. Estes S, Arnold SJ (2007) Resolving the paradox of stasis: Models with stabilizing selection explain evolutionary divergence on all timescales. *Am Nat* 169:227–244.
27. Silva M, Downing JA (1995) *CRC Handbook of Mammalian Body Masses* (CRC, Boca Raton, FL).
28. Hamilton MJ, Davidson AD, Sibly RM, Brown JH (2011) Universal scaling of production rates across mammalian lineages. *Proc R Soc Lond Ser B* 278(1705):560–566.
29. Hunt G (2007) The relative importance of directional change, random walks, and stasis in the evolution of fossil lineages. *Proc Natl Acad Sci USA* 104:18404–18408.

Supplementary Information Appendix
Evans et al. (2012) The maximum rate of evolution in mammals

Supporting Information Corrected March 5, 2012

Materials and Methods

Calculation of evolutionary rates

Clade maximum rate (CMR) examines the maximum of a phenotypic trait for a clade over evolutionary time. Fig. 1 illustrates how CMR is calculated for three clades: the green, red and blue clades. Within the green clade are five lineages, represented as broken lines. The time scale could be either individual generations, or multiple generations binned into time intervals. For the latter, the maximum of the lineage during that interval is plotted at the centre of the time interval, and maxima of adjacent time intervals are connected by a line. For each interval, the lineage with the maximum value is identified as the 'clade maximum', shown as the solid green line. The CMR is the rate of change between any pair of points along this line. In Fig. 1 the clade maximum has also been calculated for the red and blue clades, but their component lineages are not shown for clarity. The superclade of the green, red and blue clades also has a clade maximum, shown as the dashed black line. The rate of this clade maximum can be calculated in the same manner. The CMR is a conservative estimate, being a minimum estimate of the maximum rate because maximum body mass in an order at time $t + 1$, compared to the maximum body mass in the order at time t, is the minimum possible amount of change to account for the difference, occurring only if the largest species at $t + 1$ evolved from the largest species at t. If the largest species at $t + 1$ evolved from any other species at t, the rate would be higher.

We used the compilation (1) of the maximum body mass for each of 28 orders of Mammalia in each sub-epoch since 70 Ma (Mammoth database v. 1.0). We calculated rates for the mammal maximum and for the nine best sampled orders (Artiodactyla, Carnivora, Cetacea, Creodonta, Multituberculata, Perissodactyla, Primates, Proboscidea and Rodentia; the paraphyletic order Artiodactyla was analysed separately from cetaceans rather than the monophyletic Cetartiodactyla due to the very different pattern of body size increase). The mean of the natural log measurements was estimated as the natural log of the mean of untransformed measurements (2).

Cetacean body masses were estimated from a new regression equation of occipital condyle breadth (OCB, mm) vs mass (M, kg) for 18 odontocete and 11 mysticete species:

$$M = 4.924\times10^{-6}OCB^{3.858} \qquad \text{(Eq. S1)}$$

($R^2 = 0.9447$, SE = 0.2716, %PE = 55.33, %SEE = 86.89). %PE is the percent prediction error and %SEE is the percent standard error of the estimate (3, 4). Cetaceans are the only group where the maximum is found in the present day, and so underestimations of fossil taxa would result in an overestimation of the evolutionary rate. Poor sampling in the Oligocene and Early Miocene may result in underestimation of maximum size of this group, but it is unknown if this lower sampling is more extreme than for many other groups.

The maximum mass of artiodactyls in North America was calculated for 18 families and the continent as a whole for each North American Land Mammal sub-age.

For each sequence of maxima, all combinations of time points were compared. Only rates of increase in maximum size were calculated for the maximum mammalian body size, as these must be due to evolutionary change, but decreases may be due to extinctions of the previous maximum and so do not represent rates of evolution. The clade maximum rates method could also be applied to the minimum of a clade, in which case only decreases could be assessed. A

major advantage of the clade maximum metric is that a detailed phylogeny is not required, only the recognition of distinct clades.

Several methods were used to estimate body mass standard deviation (s_p). The body mass standard deviation was estimated for 64 species from eight orders from published data (5) as (ln(maximum) – ln(minimum))/4, based on an estimate that 95% of normally-distributed observations are within two standard deviations of the mean. The mean standard deviation of this estimate was 0.145, which is very similar to that of 0.15 (6) and 0.14 (7). We therefore used the value of 0.15. Using a higher estimate of 0.2 reduces all log changes in Fig. 3 by a factor of 0.125, therefore having only a small effect on the overall pattern.

For comparison, the coefficient of variation of body mass in modern mammals (8) for six species of three orders gave a mean of 0.140. The mean standard deviation for body mass estimates for fossil *Homo sapiens* (9) was 0.138. For a mass death assemblage of *Teleoceras major* where maximum and minimum body size estimates were made (10), the standard deviation was 0.070. The standard deviation for a large number of linear characters also compiled for this study was 0.054, and with an average scaling of these characters to body mass of 3 gives an estimate of the variation in body mass of 0.162.

A two-fold difference in the minimum and maximum (e.g. minimum size 1 kg, maximum size 2 kg) gives a ln standard deviation of (ln(1)-ln(2))/4 = 0.173, which is the average value for Artiodactyla.

Our results suggest that body size changes greater than 2-fold require much longer time periods. This is interesting because the range of size within a species is typically about 2-fold (ln standard deviation of mammals is 0.15, while a 2-fold range gives 0.17), suggesting that size changes >2-fold might involve evolution above the species level.

Generation time was estimated as age at first parturition (age at first reproduction plus gestation time (11)) from the data for 839 placental mammal species and for 82 marsupial species (12). Ordinary least squares regression of body mass on generation time yielded the following relationships:

$$G_{plac} = 0.175M^{0.259} \quad \text{(Eq. S2)}$$

$$G_{mars} = 0.531M^{0.091} \quad \text{(Eq. S3)}$$

where G_{plac} and G_{mars} are generation time in years for placentals and marsupials respectively and M is body mass in grams. 95% confidence intervals for the slopes of the placental and marsupial regressions are 0.247-0.272 and 0.056-0.126 respectively. This does not incorporate the effects on generation time of varying *r*- and *K*-selection strategies, but such detailed life history information is difficult to extract from the fossil record.

The generation time G of an organism is dependent on mass M according to an allometric scaling function:

$$G = b_0 M^{b_1}. \quad \text{(Eq. S4)}$$

The number of generations or biological time t_g experienced by a lineage or population is equal to the chronological time t experienced divided by generation time: $t_g = t / G$ or in differential form, $dt_g = dt / G$. Rearranging and substituting in Equation S4, we obtain

$$\frac{dt_g}{dt} = \frac{1}{b_0 M^{b_1}}. \quad \text{(Eq. S5)}$$

If mass increases exponentially with exponential rate constant α per generation, then

$$\frac{1}{M}\frac{dM}{dt_g} = \frac{d(\log M)}{dt_g} = \alpha, \quad \text{(Eq. S6)}$$

which in integrated form is

$$\log M = \alpha t_g + \log M_0, \quad \text{(Eq. S7)}$$

where M_0 is the initial body mass at $t_g = 0$.

α forms the basis for the calculation of the Haldane *h* and many other measures of evolutionary rates (e.g., $h = \alpha/s_p$, where s_p is body mass standard deviation as defined above). To get the corresponding equations for Equations S6 and S7 in terms of chronological time we note that

$$\frac{dM}{dt} = \frac{dM}{dt_g}\frac{dt_g}{dt} \quad \text{(Eq. S8)}$$

and substitute Equations S5 and S6 into Equation S8, thereby obtaining

$$\frac{dM}{dt} = \left(\frac{\alpha}{b_0}\right) M^{1-b_1}. \quad \text{(Eq. S9)}$$

The integrated solution is

$$M^{b_1} = \frac{\alpha b_1}{b_0} t + M_0^{b_1} \quad \text{(Eq. S10)}$$

This shows that M^{b_1} depends linearly on chronological time *t* with a slope *s* of $s = \alpha b_1/b_0$. Thus, the rate of change in body size per generation is

$$\alpha = \frac{s b_0}{b_1} \quad \text{(Eq. S11)}$$

and the rate of evolution of body mass can be estimated by determining through linear regression the parameters *s* and the coefficients b_0 and b_1 of the generation time allometric equation. The number of generations N_g occurring between two time points can now be obtained from Equations 6 and 11 as

$$N_g \equiv dt_g = \frac{b_1 d(\log M)}{s b_0}, \quad \text{(Eq. S12)}$$

which can be calculated for two time points and their respective masses M_1 and M_2 as

$$N_g = \left(\frac{b_1}{s b_0}\right)\left(\log M_2 - \log M_1\right). \quad \text{(Eq. S13)}$$

This calculation gives an analytically exact interpolative estimate of the interval length for that time interval. s, the slope of the time (t_y, in years) vs M^{b_1}, can be calculated as:

$$s = \frac{M_2^{b_1} - M_1^{b_1}}{t_{y_2} - t_{y_1}}. \quad \text{(Eq. S14)}$$

The pattern of increase in maximum body mass of terrestrial mammals (as $M^{0.259}$) from 70 to 30 Ma was assessed with linear ordinary least squares (stats:lm), linear segmented (segmented), Gompertz (drc), square root (nls), exponential (nls) and logistic (nls) regressions in R Statistical Environment v. 2.10.1 (13) using the packages in brackets. The OLS regression model was the best fit according to Akaiki information criterion (AIC) using the stats:AIC function (13). AIC was calculated as:

$$AIC = -2p + k \cdot npar \quad \text{(Eq. S15)}$$

where *p* is the log-likelihood, *npar* is the number of parameters in the fitted model, and $k = 2$. The log-likelihood and number of parameters for each model are indicated in Tables S1 and S3.

The pattern of increase in $M^{0.259}$ maximum size for seven orders from their origin to their maximum was also assessed using OLS linear regression (Table 1). The pattern of increase in cetaceans was examined for the period of the Oligocene to the Recent as the increase to the first local maximum (*Basilosaurus*) is represented by only a single time interval. In addition to using a generation scaling coefficient of 0.259, all analyses were also repeated with a generation scaling coefficient of 0.25 (Tables S2 and S3).

Reference database of evolutionary rates

We calculated evolutionary rates for mammal data in references that cited previous compilations (6, 14, 15) and others where sufficient data were present in the original paper to allow estimation of body mass and time intervals. Table S4 lists the sources of data for body size, generation time and interval length for the studies used. Data quality for these sources will be variable, depending on factors such as the accuracy of the identification of ancestor-descendant pairs and the date at which the derived morphology was actually attained. Nonetheless we have confidence in the general pattern of results that depend on them.

For most references, generation times and interval lengths were calculated as per maximum size. For others, the generation times have been estimated from a method other than directly from the body mass-generation time regression (for example, where the authors themselves or another author since has estimated the generation time), and these were used to calculate interval length in number of generations:

$$N_g = \frac{t_{y_2} - t_{y_1}}{\sqrt{G_2 G_1}}, \qquad \text{(Eq. S16)}$$

where G_1 and G_2 are the generational times at times 1 and 2 respectively, giving the geometric mean of the start and end generation times. For small changes in body mass (e.g. <10-fold change) the differences in the interval lengths calculated by the two methods are minor (<2%).

Random walk simulations

Several sensitivity tests were conducted to examine whether the incompleteness of the fossil record and/or binning data by sub-epoch biased rate calculations. We conducted a random walk simulation with various levels of preservation. Each simulation comprised 100 independent random walks, with the movement up or down at each of the 1000 steps drawn from a normal distribution of mean 0, s.d. 1. The walks were divided into 10 subclades, and time was divided into 10 intervals. The maximum within each subclade and for the whole clade was calculated for each interval. The rates of change in the subclade and clade maxima were calculated per interval. The process of fossilization was simulated by downsampling the data to between 1% and 0.005% of all steps in all walks. Maxima in each interval and rates of change were then calculated for each subclade and clade. One hundred simulations were run with different sets of walks. 95% confidence intervals of rates for the full and fossilized datasets over all simulations were compared to see whether the fossilisation process gave a biased higher or lower estimate of the true rates (Table S5). This indicated that the estimated evolutionary rates are not significantly biased due to these effects, although at very low preservation levels variation in measured rates increased.

Examples of island dwarfism

The key examples of large decreases examined here are instances of island dwarfism, the Jersey red deer (16) and insular pygmy elephantids (17-19). These are the only examples of large change (over half an order of magnitude) for which body mass estimates have been made and there is some estimation of the timing of the split from the large ancestral species. The Jersey deer represents a change from about 200 kg to 36 kg during a maximum of 5800 years (16). As this is a maximum estimate of the divergence time, this will represent a minimum and therefore conservative estimate of the evolutionary rate.

Three examples of pygmy or dwarf elephants are examined here. The first is the pygmy elephant (*Elephas falconeri*) that evolved on Sicily and Malta, with an estimated mass of 100 kg (17). *Elephas falconeri* was probably a descendant of *E.antiquus*, which weighed approximately 10,000 kg (20). Second, the Cyprus pygmy elephant (*Elephas cypriotes*) weighed around 200 kg (18) and was also probably descended from *E. antiquus*. We have used an estimate of 800,000 years as the divergence time between *E. antiquus* and each of *E. falconeri* and *E. cypriotes*, as *E. antiquus* did not arrive in Europe until the start of the Middle Pleistocene (0.8 Ma) (61). Third is the California Channel Islands mammoth (*Mammuthus exilis*) of about 1,000 kg, derived from the mainland *Mammuthus columbi* (around 10,000 kg). The dwarf mammoth would have evolved in less than 85,000 years (19).

The Mediterranean proboscidean pygmies represent the greatest change in body mass for insular dwarfism that we are aware of, at up to 2 orders of magnitude between ancestor and descendant. If the dates of divergence differ from the estimated range of 0.8 million years, the horizontal position of the point in Fig. 3 will move but not the vertical.

Asymmetry of increases and decreases

The apparent asymmetry between rates of increases and decreases would be falsified if fossil evidence of rapid gigantism were found. We expect that it would be easier to find examples of gigantism compared to dwarfism in the fossil record due to the bias of finding larger fossils compared to small ones. For instance, even at a distance of 65 million years, dwarfed, presumably island forms of dinosaurs have been recognized in the Haţeg basin (21), but no instances of such dramatic insular gigantism in mammals are known. Examples such as the giant rabbit of Minorca (22) are undated, and represent less than one order of magnitude change from a probable ancestor.

Figures

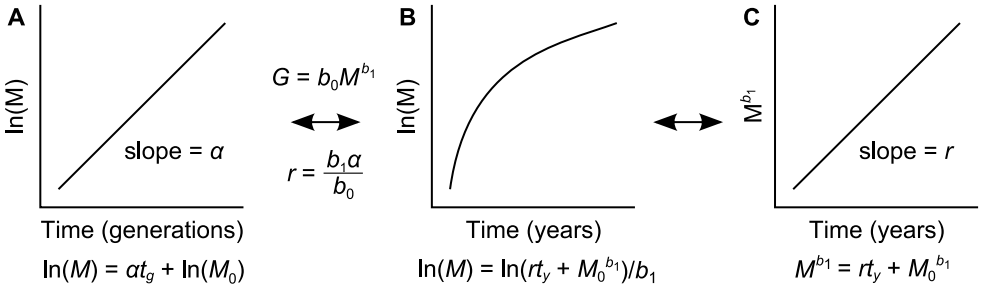

Fig. S1. Exponential increase in body size in biological time is curvilinear in chronological time but linear when mass is scaled to account for generation time. **(A)** When evolutionary increase in body size (M) is exponential over biological time (in generations t_g), change in log mass is linear. **(B)** Assuming that generation time (G) increases with mass, $G = b_0 M^{b_1}$, log mass shows a slowing in the rate of increase in body size in chronological time (in years t_y). **(C)** When M^{b_1} is plotted versus chronological time, this trajectory is linear with a slope r. The rate of increase per generation α can be calculated from the slope r by multiplying by b_0/b_1.

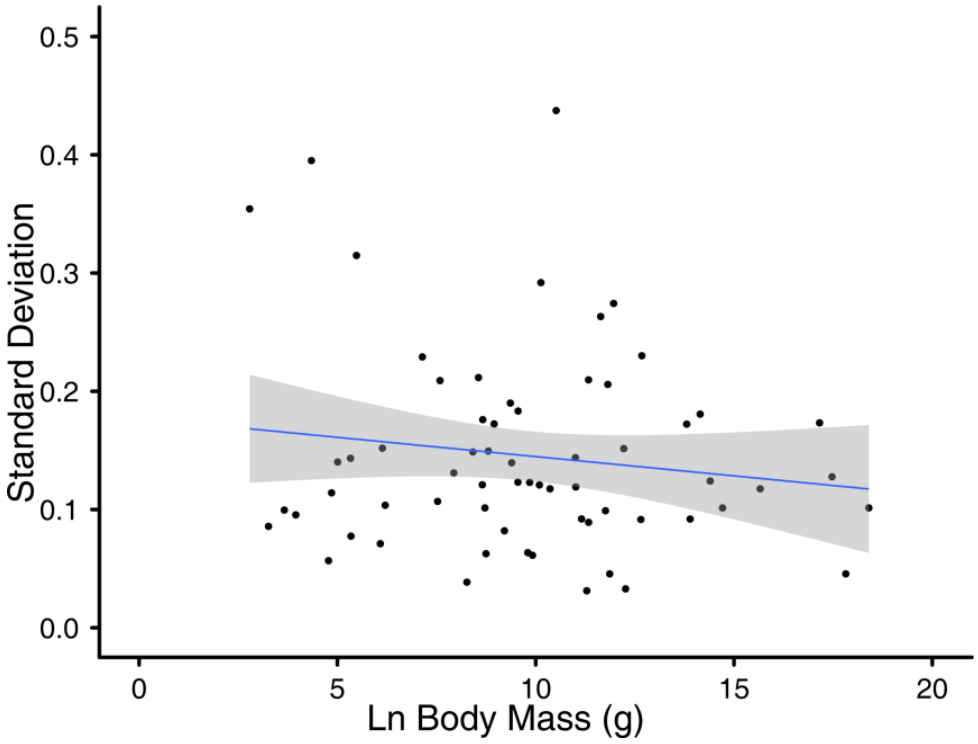

Fig. S2. Ln body mass vs standard deviation for 64 species of modern mammals (*30*). Mean ± S.E. = 0.145 ± 0.011, 95% Confidence Interval = 0.124 to 0.167.

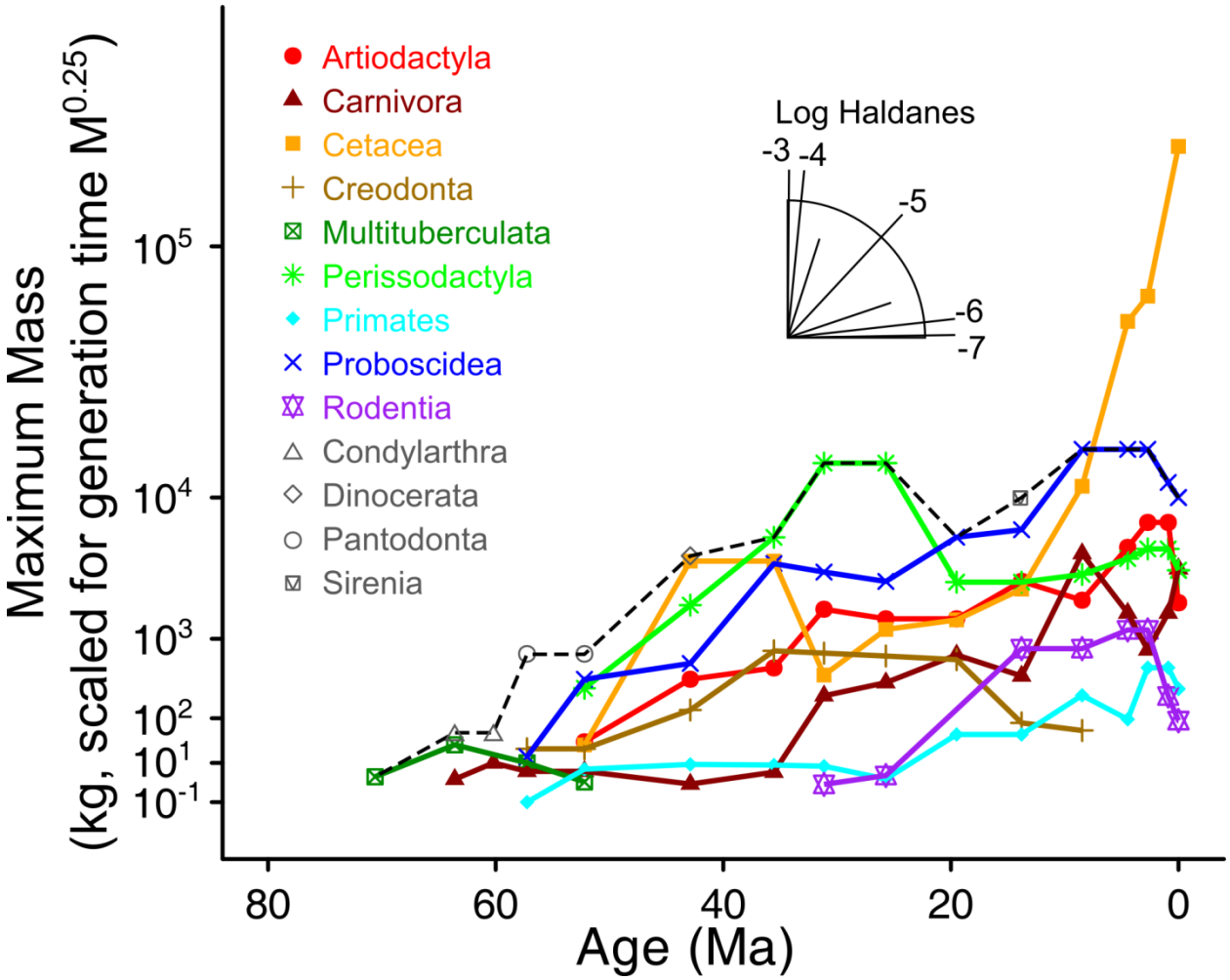

Fig. S3. Maximum mammalian body mass over time for terrestrial mammals (dashed black line) and separate mammal orders (colored lines). Mass is scaled to the power of 0.25 on the y axis (given a theoretical $M^{0.25}$ scaling of generation times), so the slope of lines indicates generation time-corrected evolutionary rates as indicated by angular scale (haldanometer). This shows that there is no major difference in the pattern when the theoretical expected value of 0.25 is used rather than the empirical scaling coefficient of 0.259 for generation time to body mass.

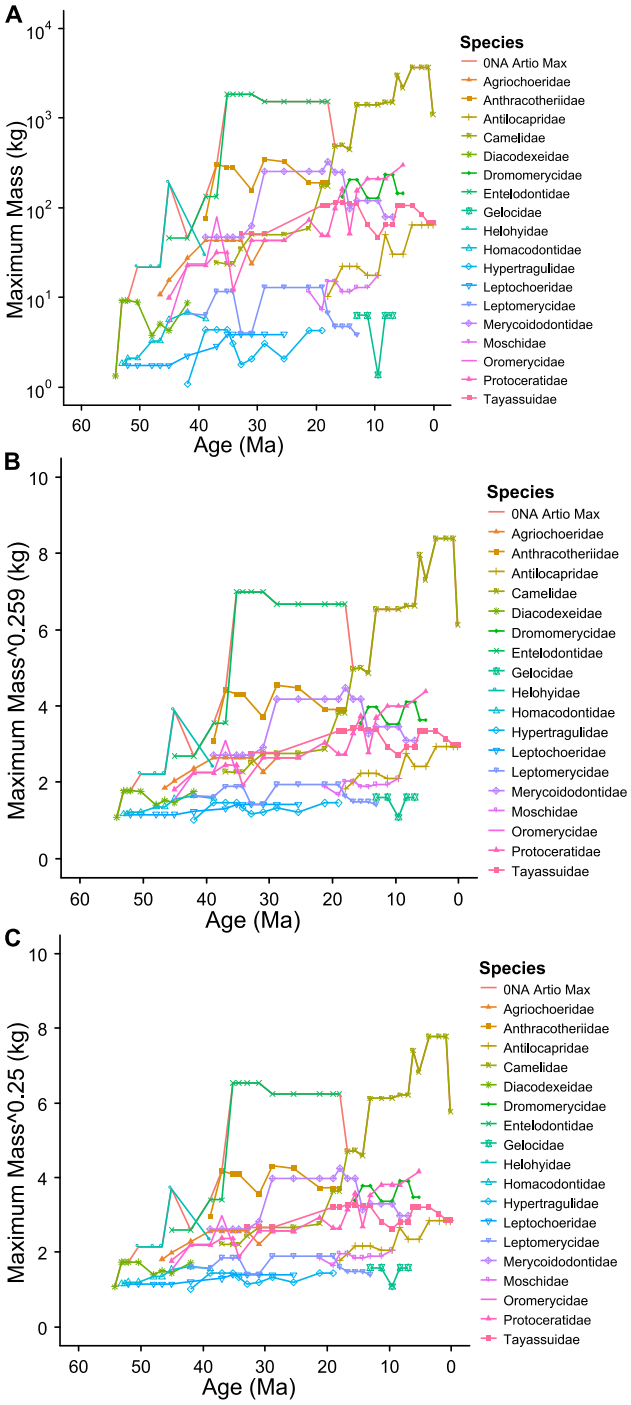

Fig. S4. Maximum body mass over time for North American artiodactyls for **(A)** log(M), **(B)** $M^{0.259}$ and **(C)** $M^{0.25}$.

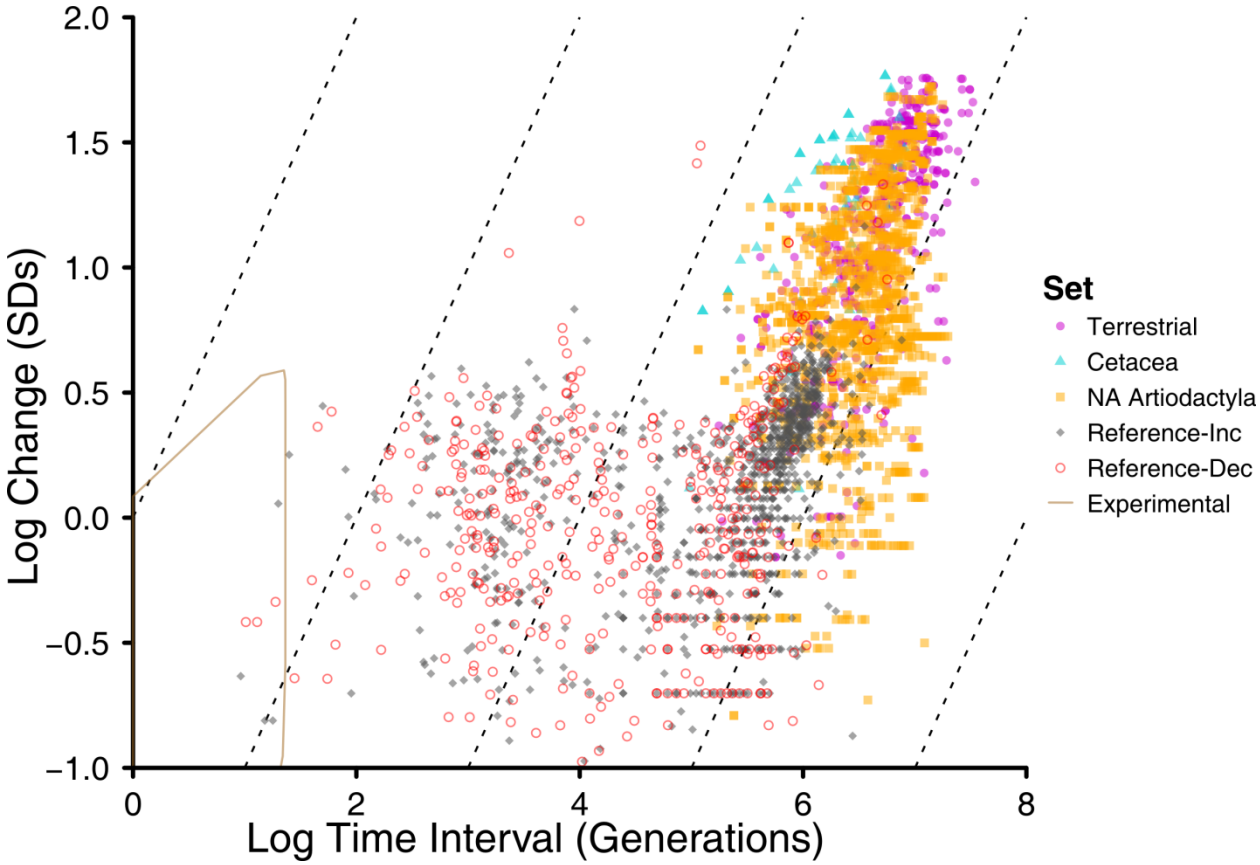

Fig. S5. Individual rate calculations for interval vs change for all datasets examined. Fig. 3 was generated by calculating minimum convex polygons of these data. For the experimental data, only the minimum convex polygon of the published data were available (*3*, *14*).

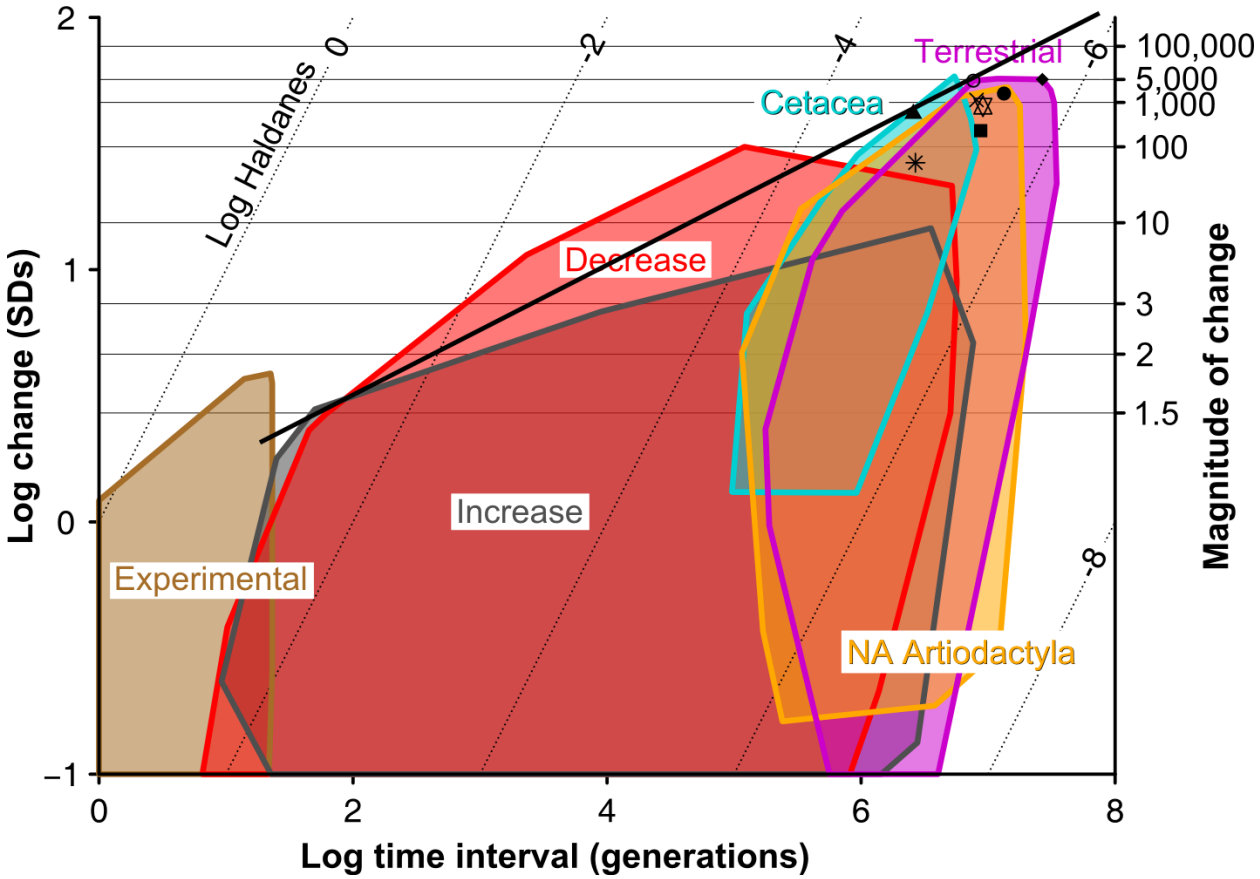

Fig. S6. Maximum rate of body mass increase scales as ~0.25 of interval length. Extrapolating this relationship predicts that an interval of about 24 million years is required for a mouse-to-elephant body size transformation (100,0000-fold).

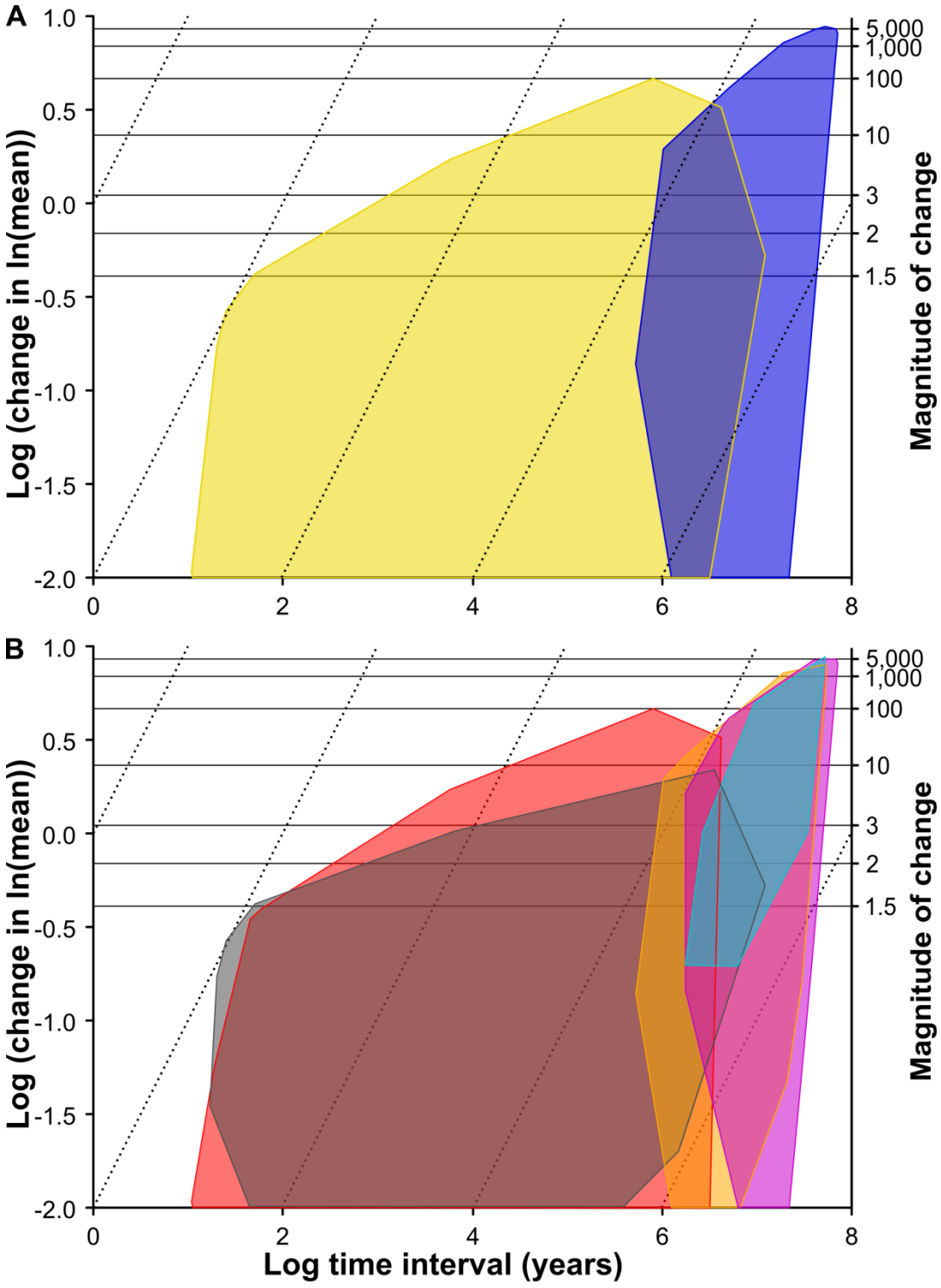

Fig. S7. Rates of evolution for large changes in mammalian body mass with change in log(difference in ln(mean)) and time interval in years. This gives evolutionary rate in darwins, plotted as isodarwins (diagonal dotted lines). Color scheme as in Fig. 3. Experimental rates are not calculated here as intervals were only given in generations, not years.

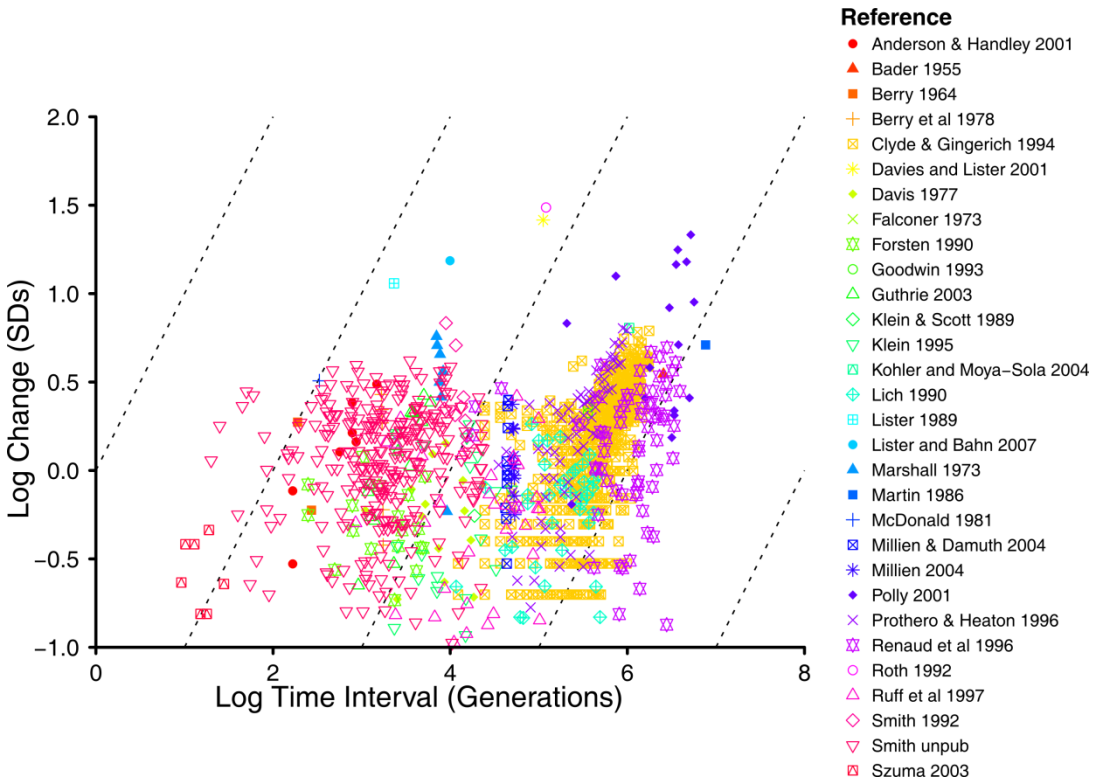

Fig. S8. Change vs time interval for reference database showing data separately for each study.

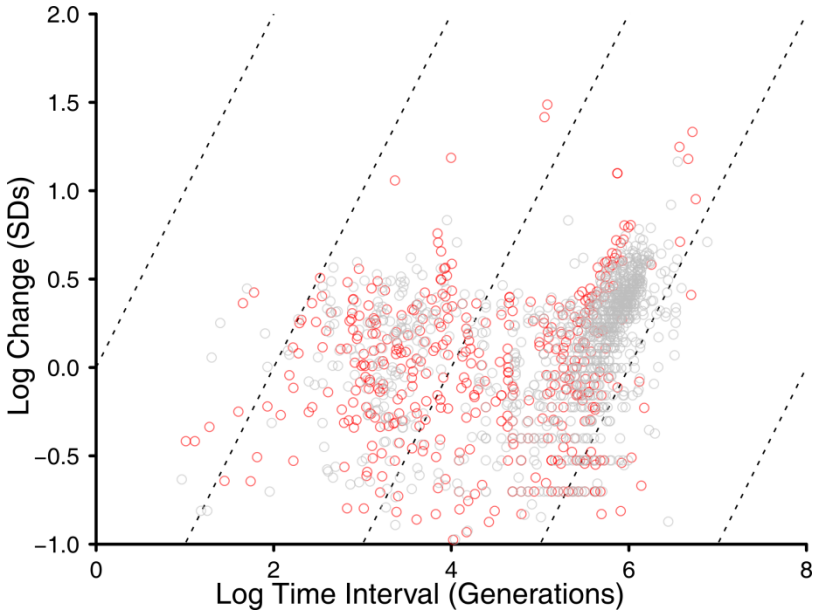

Fig. S9. Change vs time interval for reference database showing negative (red) and positive (gray) change.

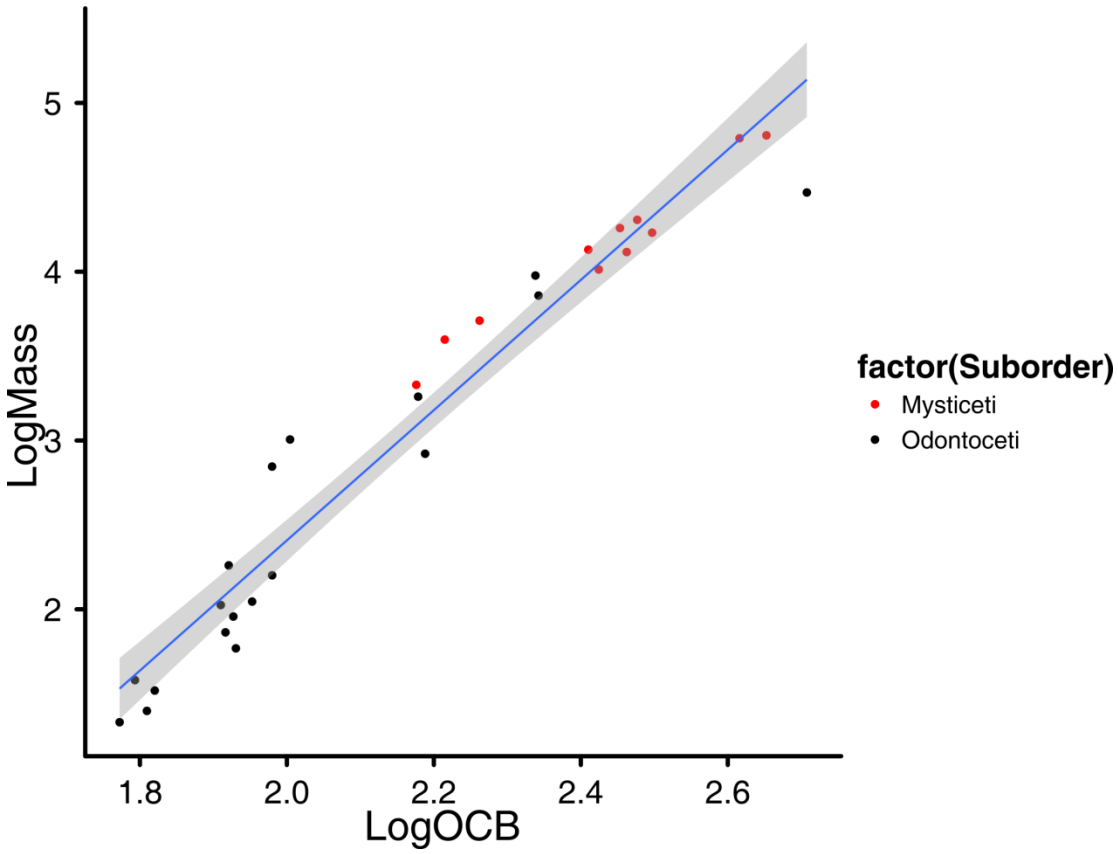

Fig. S10. Log(Mass) vs Log(OCB) for 18 odontocete and 11 mysticete species.

A

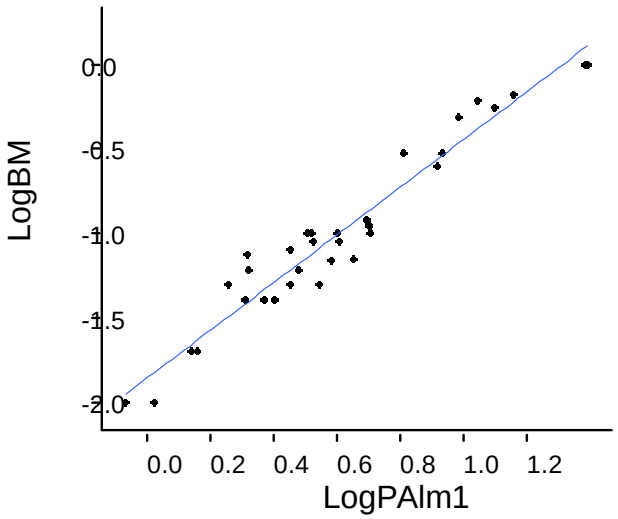

B

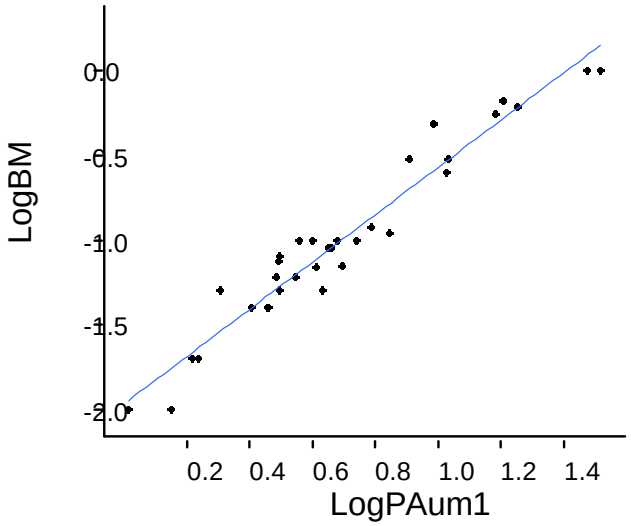

Fig. S11. Regression of upper (A) and lower (B) first molar log(planar tooth area) vs log(body mass) for 33 species of murid rodents for estimation of body mass for Ref. (23).

Tables

Table S1. Comparison of models for maximum body mass of terrestrial mammals ($M^{0.259}$) from 70 to 30 Ma using Akaike information criterion (AIC) showing log-likelihood and number of parameters (*npar*) for each model.

Model	**AIC**	log-likelihood	*npar*
OLS	50.27	-22.14	3
Segmented	53.73	-21.86	5
Gompertz	52.21	-22.1	4
Square root	60.7	-28.35	2
Exponential	53.75	-23.88	3
Logistic	52.99	-22.49	4

Table S2. The maximum body mass for all terrestrial mammals and for several orders increased linearly when generation time is accounted for. Slope for linear regression of $M^{0.25}$ vs Age (Ma) for each group from their origin until their maximum (except for Cetacea, which is for the period of 31 Ma to the Recent). The average rate in haldanes was calculated using the mammalian scaling relationship of generation time with body mass.

	Slope	**Haldanes ($\times 10^{-6}$)**	**R^2**	***P***
Terrestrial maximum	1.35	6.09	0.97	1.12×10^{-5}
Artiodactyla	0.63	2.84	0.90	3.33×10^{-5}
Carnivora	0.57	2.54	0.74	6.47×10^{-4}
Cetacea	2.71	12.20	0.83	1.58×10^{-3}
Perissodactyla	1.80	8.08	0.98	9.04×10^{-3}
Primates	0.35	1.55	0.78	1.35×10^{-4}
Proboscidea	0.92	4.11	0.91	6.46×10^{-5}
Rodentia	1.06	4.74	0.93	1.77×10^{-3}

Table S3. Comparison of models for maximum body mass of terrestrial mammals ($M^{0.25}$) from 70 to 30 Ma using Akaike information criterion (AIC) showing log-likelihood and number of parameters (*npar*) for each model.

Model	**AIC**	log-likelihood	*npar*
OLS	47.61	-20.8	3
Segmented	51.21	-20.61	5
Gompertz	49.64	-20.82	4
Square root	57.76	-26.88	2
Exponential	51.79	-22.9	3
Logistic	50.39	-21.19	4

Table S4. Studies used in reference database of mammalian body size evolutionary rates. Figure, Table and page references refer to the reference in the Reference column unless otherwise noted. M_1, first lower molar; M_2, second lower molar; M_3, third lower molar; M^3, third upper molar.

Reference	Taxa	Measure	Body Mass Estimation	Generation Time	Ages/Intervals
(24)	*Bradypus*	Body mass (Table 2)	Estimated in Table 2	6 years (25)	Estimated divergence of islands given on pp. 3-5
(26)	*Merychyus*	Mean basal length (Table 1)	Appendix Table 16.8 BCL (27)	Regression from body mass for placentals (12)	One interval estimated at 12 million years on p. 120
(28)	*Mus musculus*	Body mass of males (Table 6)	Given in Table 6	Regression from body mass for placentals (12)	Estimated intervals 70 years (Skokholm) and 100 years (May)
(29)	*Mus musculus*	Body mass (mean of male and female means) (Table II)	Given in Table II	Regression from body mass for placentals (12)	One interval of 625 years on p. 76
(30)	*Cantius*	Mean ln(M_1 area) (ln(M_1 length)+ln(M_1 width)) (Appendix 1)	Table 3 ln(M_1 area) (31)	1 year (estimated on p. 510)	Section level in metres; average sedimentary accumulation rate of 2450 yr/m in Appendix 1
(18)	*Elephas antiquus*-*Elephas cypriotes*	Body mass (p. 479)	*E. antiquus* estimated at 10,000 kg (20); *E. cypriotes* estimated at 200 kg (18)	Regression from body mass for placentals (12)	One interval of 2 million years (see notes above)
(32)	*Vulpes vulpes*	Mean M_1 length (Table II)	Table 16.6 Canidae M1L (4)	Regression from body mass for placentals (12)	Estimated dates in Table I
(33)	Equids	Mean M_1or M_2 length at tooth base (Table 1)	Appendix Table 16.8 Perissodactyls and hyracoids only M_1 length (27)	3 years (11)	Estimated by (11)
(34)	*Cynomys*	Mean M_1 length × width (Table 7.3)	All mammals M_1 (35)	Regression from body mass for placentals (12)	Estimated ages given in Table 7.4
(36)	Equids	Mean metatarsal length (Supplementary Information)	Appendix Table 16.7 Equids MT1 (37)	Regression from body mass for placentals (12)	Data grouped into 5000 year intervals starting at 37500 yr.b.p
(38)	Gazelles	Mean of humerus distal medio-lateral diameter (Fig. 20.1) and mean of M_3 length (Fig. 20.2)	Appendix Table 16.7 Bovids Only H5 (37); Appendix Table 16.9 All selenodonts M_3 length (27)	Regression from body mass for placentals (12)	Average age of time periods given in Fig. 20.1

(39)	*Crocuta crocuta*	Mean M_1 (Table 1)	Table 16.6 Total sample M1L (4)	Regression from body mass for placentals (12)	Time periods given on p. 90
(40)	*Myotragus*	Body mass (p. 126)	Estimated on p. 126	Regression from body mass for placentals (12)	One interval estimated at 2.8 million years on p. 126
(41)	*Cosomys primus*	Mean M_1 length (Table 1)	Appendix Table 16.11 Cricetine rodents (42)	1/3 year (11)	Elevations given in feet; average sediment accumulation of 1.8 feet per ky(11)
(16)	*Cervus elephas*	Body mass (p. 540)	Estimated on p. 540	2.5 years (11)	One interval of 5800 years on p. 541
(19)	*Mammuthus*	Body mass (p. 38)	Estimated on p. 38	Regression from body mass for placentals (12)	One interval of 85,000 years on p. 38
(43)	Marsupials	Mean M^3 or M_3 length (Tables 67A, 75A, 46A, 67, 62, 47, 44A, 46, 22A, 28A); Table 2 (44); Table 1 (45)	*Macropus*: Appendix Table 16.12 TUML (27); *Petrogale* Appendix Table 16.12 TLML (27); *Sarcophilus* and *Dasyurus* Fig. 5 M3L (46)	Regression from body mass for marsupials (12)	One interval estimated at 10,000 years on p. 409
(47)	*Sigmodon*	Ln Mean M_1 length (Fig. 1)	Equation 1	Regression from body mass for placentals (12)	One interval estimated at 3.8 million years from Fig. 1
(48)	*Bison*	Mean femur rotational length for males and females (Tables 22 and 30)	Appendix Table 16.7 Bovids Only F1 average of males and females (37)	3 years (11)	Estimate of 1000 year interval between *B. a. antiquus* and *B. b. bison*(11)
(49)	*Apodemus argenteus*	Mean anterior-posterior diameter of lower incisor (Table 1)	Anterior-posterior diameter of lower incisor (Table 3) (50)	Regression from body mass for placentals (12)	Estimated divergence of island at LGM at 0.021 Ma on p. 1270
(51)	*Apodemus speciosus*	Mean anterior-posterior diameter of lower incisor (Table 1)	Anterior-posterior diameter of lower incisor (Table 3) (50)	Regression from body mass for placentals(12)	Estimated divergence of island at LGM at 0.021 Ma on p. 1355
(52)	Viverravids	Body mass (Fig. 2)	Estimated in Fig. 2	Estimated in Fig. 2	Given in Fig. 2
(53)	*Miniochoerus*	Mean M^{1-3} length (Fig. 2)	Appendix Table 16.9 Nonselenodonts M^{1-3} length(27)	Regression from body mass for placentals (12)	Interpolated from regression of feet and age based on dating of three levels (Fig. 2)

(23)	*Stephanomys*	Mean M^1 and M_1 area (Appendices 1 and 2)	Mean of regressions of M^1 and M_1 area from data in Fig. S11 (present paper): log(M) = 1.362*(UM1A)-1.95; log(M) = 1.404*(LM1A)-1.86	Regression from body mass for placentals (12)	Intervals read from Fig. 1
(17)	*Mammuthus primigenius-Elephas falconeri*	Body mass (Fig. 9.4)	*M. primigenius* estimated at 5000 kg (20); *E. falconeri* estimated at 100 kg in Table 3	Regression from body mass for placentals (12)	One time interval of 0.5 million years (see notes above)
(9)	*Homo sapiens*	Mean body mass (Table 1)	Derived from regression of femoral head and/or stature/bi-iliac breadth (mean taken if both proxies used) in modern and Pleistocene *Homo* (Fig. 1)	14.5 years (54)	Ages given in Table 1
(55)	*Neotoma*	Mean body length (Table 1)	Formula in Fig. 4	Regression from body mass for placentals (12)	Times of island isolation given in Table 2
(56-59)	*Neotoma*	Mean of 10 largest pellets for Atlatl Cave (NM), Bison Alcove (UT), Fishmouth Cave (UT), Lyman Lake (AZ), Pryor Mountains (WY), Rocky Canyon (UT) and Southern Bighorn Mountains, East Pryor (MT), USA	Fig. 3 equation (59)	Estimated at 1 year (F.A. Smith)	Ages in midden sequences in years
(60)	*Vulpes vulpes*	Mean M_1 length (Table 2)	Table 16.6 Canidae M1L (4)	Regression from body mass for placentals (12)	Ages of periods given on p. 49

Table S5. Fossilization slightly reduces the measured evolutionary rates compared to the full dataset. Means and 95% confidence intervals for clade maxima rates for clades and subclades for maximum preservation rate (*PR* = 100%) and six levels of preservation rate (*PR* = 1.0 to 0.005%). For PR < 0.05%, some intervals had no fossils present (percentage of intervals with no fossils preserved *NFP*) and so represent a very poor fossil record.

	***PR* (%)**	**Mean**	**2.5%**	**97.5%**	***NFP* (%)**
Clade rates	100	0.0639	-0.0747	0.2153	0
	1.0	0.0638	-0.0768	0.2154	0
	0.5	0.0643	-0.0744	0.2117	0
	0.1	0.0643	-0.0850	0.2199	0
	0.05	0.0604	-0.1811	0.2978	0
	0.01	0.0561	-0.2227	0.3431	0
	0.005	0.0400	-0.3306	0.4498	0
Subclade rates	100	0.0403	-0.1026	0.1907	0
	1.0	0.0403	-0.1031	0.1918	0
	0.5	0.0406	-0.1063	0.1958	0
	0.1	0.0404	-0.1141	0.2065	0
	0.05	0.0348	-0.2945	0.3490	0
	0.01	0.0261	-0.4277	0.4739	4.44
	0.005	0.0005	-0.6024	0.5245	58.89

Table S6. Maximum body size for terrestrial mammals and nine mammalian orders. Log change (SD) and log interval (generations) are shown for positive changes in body size for each time point compared to the next time point. For Fig. 3, all combinations of time points in a series were compared.

Order	Species	Maximum Mass (Kg)	Age (Ma)	Gene-ration Time (yr)	Log Change (SD)	Log Interval (Gen)
Terrestrial mammals						
Proboscidea	*Loxodonta africana*	10000	0.00005	11.345		
Proboscidea	*Loxodonta africana*	10000	0.005	11.345		
Proboscidea	*Elephas recki/Mammuthus columbi/Mammuthus trogontherii*	12000	0.9035	12.602		
Proboscidea	*Deinotherium bozasi*	17450	2.703	13.105		
Proboscidea	*Deinotherium bozasi/giganteum*	17450	4.465	13.105		
Proboscidea	*Deinotherium bozasi/giganteum*	17450	8.47	13.105		
Proboscidea	*Gomphotherium productum*	6568	13.79	10.175	0.814	5.662
Proboscidea	*Prodeinotherium bavaricum*	5917	19.5	9.904	-0.157	5.755
Perissodactyla	*Indricotherium transouralicum*	15000	25.715	12.602		
Perissodactyla	*Indricotherium transouralicum*	15000	31.15	12.602		
Perissodactyla	*Brontops dispar*	5907	35.55	9.899	0.793	5.594
Dinocerata	*Uintatherium* sp.	4500	42.9	9.226	0.259	5.886
Pantodonta	*Coryphodon lobatus*	700	52.2	5.698	1.094	6.104
Pantodonta	*Coryphodon lobatus*	700	57.25	5.698		
Condylarthra	*Ectoconus* sp.	54.2	60.2	2.937	1.232	5.85
Condylarthra	*Ectoconus* sp.	54.2	63.6	2.937		
Multituberculata	*Meniscoessus robustus*	3.3	70.6	1.423	1.271	6.525
Orders						
Artiodactyla	*Hippopotamus amphibius*	2065	0.00005	6.84		
Artiodactyla	*Hippopotamus amphibius*	2065	0.005	6.84		
Artiodactyla	*Hippopotamus gorgops*	7255	0.9035	10.441		
Artiodactyla	*Hippopotamus gorgops*	7255	2.703	10.441		
Artiodactyla	*Hippopotamus gorgops*	5114	4.465	9.536	0.368	5.247
Artiodactyla	*Megacamelus merriami*	2162	8.47	7.63	0.759	5.671
Artiodactyla	*Megatylopus matthewi*	3005	13.79	8.31		
Artiodactyla	*Daeodon hollandi*	1519	19.5	6.964	0.658	5.875
Artiodactyla	*Daeodon hollandi*	1519	25.715	6.964		
Artiodactyla	*Archaeotherium* sp.	1829	31.15	7.307		
Artiodactyla	*Entelodon* sp.	497	35.55	5.214	0.939	5.851
Artiodactyla	*Anthracotherium pangan*	365	42.9	4.813	0.313	6.166
Artiodactyla	*Bunophorus Bunophorus*	35	52.2	2.623	1.194	6.411
Carnivora	*Mirounga leonina*	3692	0.00005	7.058		

Carnivora	*Mirounga leonina*	3692	0.005	7.058		
Carnivora	*Odobenus rosmarus*	1700	0.9035	7.17		
Carnivora	*Arctodus simus*	776	2.703	5.852	0.718	5.443
Carnivora	*Valenictus chulavistensis*	1700	4.465	7.17		
Carnivora	*Pontolis magnus*	4665	8.47	9.312		
Carnivora	*Amphicyon ingens*	400	13.79	4.929	1.214	5.888
Carnivora	*Phoberocyon johnhenryi*	689.3	19.5	5.675		
Carnivora	*Amphicyon ulungurensis*	331	25.715	4.693	0.689	6.08
Carnivora	*Quercylurus* sp.	221.6	31.15	4.23	0.427	6.086
Carnivora	*Daphoenus lambei*	4.94	35.55	1.579	1.404	6.214
Carnivora	*Procynodictis vulpiceps*	1.59	42.9	1.178	0.877	6.73
Carnivora	*Didymictis proteus*	5.3	52.2	1.608		
Carnivora	*Didymictis proteus*	5.3	57.25	1.608		
Carnivora	*Miacoid carnivore*	10	60.2	1.896		
Carnivora	*Protictis simpsoni*	2.61	63.6	1.339	0.952	6.327
Cetacea	*Balaenoptera musculus*	190000	0.00005	24.323		
Cetacea	*Balaenoptera musculus*	190000	0.005	24.323		
Cetacea	*Balaenoptera* sp.	69540	2.703	18.748	0.826	5.1
Cetacea	*Physeter macrocephalus*	57100	4.465	17.815	0.119	4.984
Cetacea	*Mixocetus elysius*	11476.28	8.47	11.757	1.029	5.439
Cetacea	*Pelocetus calvertensis*	2633.97	13.79	8.031	0.992	5.736
Cetacea	*Aglaocetus moreni*	1487.23	19.5	6.926	0.581	5.884
Cetacea	*Micromysticetus tobieni*	1223.05	25.715	6.584	0.115	5.964
Cetacea	Aetiocetidae USNM314627	410.08	31.15	4.961	0.862	5.977
Cetacea	*Basilosaurus cetoides*	4158.8	35.55	9.039		
Cetacea	*Basilosaurus cetoides*	4158.8	42.9	9.039		
Cetacea	*Pakicetus attocki*	29.7	52.2	2.513	1.518	6.261
Creodonta	*Dissopsalis carnifex*	60	8.47	3.016		
Creodonta	*Dissopsalis pyroclasticus*	83	13.79	3.28		
Creodonta	*Megistotherium osteothalestes*	614	19.5	5.507		
Creodonta	*Hyaenodon weilini/gigas*	671	25.715	5.636		
Creodonta	*Hyaenodon gigas*	720	31.15	5.739		
Creodonta	*Hemipsalodon* sp.	760	35.55	5.82		
Creodonta	*Patriofelis* sp.	136.5	42.9	3.731	1.059	6.194
Creodonta	*Palaeonictis peloria*	24.07	52.2	2.38	1.063	6.491
Creodonta	*Palaeonictis peloria*	24.07	57.25	2.38		
Multituberculata	*Neoliotomus ultimus*	2	52.2	1.25		
Multituberculata	*Sphenopsalis nobilis*	10	57.25	1.896		
Multituberculata	*Taeniolabis taoensis*	30	63.6	2.52		
Multituberculata	*Meniscoessus robustus*	3.3	70.6	1.423	1.168	6.562

Perissodactyla	*Ceratotherium simum*	3600	0.00005	8.27		
Perissodactyla	*Ceratotherium simum*	3600	0.005	8.27		
Perissodactyla	*Elasmotherium sibiricum*	5000	0.9035	9.481		
Perissodactyla	*Elasmotherium sibiricum*	5000	2.703	9.481		
Perissodactyla	*Aphelops mutilus*	4325	4.465	9.131	-0.015	5.277
Perissodactyla	*Iranotherium morgani*	3366	8.47	8.557	0.223	5.656
Perissodactyla	*Teleoceras medicornutum*	2965	13.79	8.281	-0.073	5.801
Perissodactyla	*Teleoceras medicornutum*	2965	19.5	8.281		
Perissodactyla	*Indricotherium transouralicum*	15000	25.715	12.602		
Perissodactyla	*Indricotherium transouralicum*	15000	31.15	12.602		
Perissodactyla	*Brontops dispar*	5907	35.55	9.899	0.793	5.594
Perissodactyla	*Telmatherium altidens*	1975	42.9	7.454	0.864	5.931
Perissodactyla	*Lophiodon rhinoceroides*	280	52.2	4.494	1.115	6.201
Primates	*Gorilla beringei graueri*	275	0.00005	4.247		
Primates	*Gorilla beringei graueri*	275	0.005	4.247		
Primates	*Gigantopithecus blacki*	500	0.9035	5.222		
Primates	*Gigantopithecus blacki*	500	2.703	5.222		
Primates	*Theropithecus (Simopithecus) oswaldi*	96	4.465	3.406	1.041	5.618
Primates	*Gigantopithecus blacki*	225	8.47	4.247		
Primates	*Afropithecus turkanensis/Graecopithecus freybergi*	50	13.79	2.876	1.001	6.18
Primates	*Afropithecus turkanensis/Proconsul major*	50	19.5	2.876		
Primates	*Dolichocebus gaimanensis*	2.7	25.715	1.351	1.289	6.488
Primates	*Aegyptopithecus zeuxis*	7.9	31.15	1.784		
Primates	*Amphipithecus mogaungensis*	8.6	35.55	1.823		
Primates	*Pondaungia* sp.	9	42.9	1.845		
Primates	*Pelycodus danielsae*	6.3	52.2	1.682	0.376	6.722
Primates	*Atiatlasius koulchii*	0.1	57.25	0.575	1.441	6.69
Proboscidea	*Loxodonta africana*	10000	0.00005	11.345		
Proboscidea	*Loxodonta africana*	10000	0.005	11.345		
Proboscidea	*Mammuthus trogontotherii*	15000	0.9035	12.602		
Proboscidea	*Deinotherium bozasi*	17450	2.703	13.105		
Proboscidea	*Deinotherium bozasi/giganteum*	17450	4.465	13.105		
Proboscidea	*Deinotherium bozasi/giganteum*	17450	8.47	13.105		
Proboscidea	*Gomphotherium productum*	6568	13.79	10.175	0.814	5.662
Proboscidea	*Prodeinotherium bavaricum*	5917	19.5	9.904	-0.157	5.755
Proboscidea	*Palaeomastodon beadnelli*	3000	25.715	8.306	0.656	5.835
Proboscidea	*Barytherium grave*	3500	31.15	8.644		
Proboscidea	*Barytherium* sp.	4000	35.55	8.949		

Proboscidea	*Numidotherium koholense*	558	42.9	5.373	1.118	6.021
Proboscidea	*Daouitherium rebouli*	364	52.2	4.81	0.455	6.262
Proboscidea	*Phosphatherium* sp.	15	57.25	2.106	1.328	6.188
Rodentia	*Hydrochoerus hydrochaeris*	91	0.00005	3.016		
Rodentia	*Hydrochoerus hydrochaeris*	91	0.005	3.016		
Rodentia	*Castoroides ohioensis*	220	0.9035	4.222		
Rodentia	*Josephoartigasia monesi*	1211	2.703	6.567		
Rodentia	*Josephoartigasia monesi*	1211	4.465	6.567		
Rodentia	*Phoberomys insolita*	800	8.47	5.898	0.442	5.808
Rodentia	*Phoberomys insolita*	800	13.79	5.898		
Rodentia	*Neoreomys* sp.	3.7	25.715	1.465		
Rodentia	Dasyproctidae	1.54	31.15	1.167	0.768	6.618

Table S7. Maximum body mass for North American artiodactyls and 18 families. Log change (SD) and log interval (generations) are shown for positive changes in body size for each time point compared to the next time point. For Fig. 3, all combinations of time points in a series were compared.

Family	Species	Maximum Mass (Kg)	Age (Ma)	Gene-ration Time (yr)	Log Change (SD)	Log Interval (Gen)
Camelidae	*Camelops hesternus*	1100	0.125	6.405		
Camelidae	*Gigantocamelus spatulus*	3674	0.875	8.754		
Camelidae	*Gigantocamelus spatulus*	3674	2	8.754		
Camelidae	*Gigantocamelus spatulus*	3674	3.625	8.754		
Camelidae	*Megacamelus merriami*	2162	5.25	7.63	0.548	5.298
Camelidae	*Megatylopus matthewi*	3005	6.125	8.31		
Camelidae	*Megatylopus gigas*	1486	7	6.924	0.672	5.061
Camelidae	*Megatylopus gigas*	1486	8.25	6.924		
Camelidae	*Megatylopus primaevus*	1400	9.5	6.818	-0.401	5.26
Camelidae	*Megatylopus* sp.	1400	11.25	6.818		
Camelidae	*Megatylopus* sp.	1400	13.05	6.818		
Camelidae	*Aepycamelus robustus*	446	14.3	5.07	0.882	5.326
Camelidae	*Procamelus leptocolon*	500	15.5	5.222		
Camelidae	*Aepycamelus procerus*	488	16.75	5.189	-0.791	5.38
Entelodontidae	*Daeodon hollandi*	1519	18	6.964		
Entelodontidae	*Daeodon hollandi*	1519	19	6.964		
Entelodontidae	*Daeodon hollandi*	1519	21.25	6.964		
Entelodontidae	*Daeodon hollandi*	1519	25.445	6.964		
Entelodontidae	*Daeodon hollandi*	1519	28.82	6.964		
Entelodontidae	*Megachoerus latidens*	1829	31	7.307		
Entelodontidae	*Megachoerus latidens*	1829	32.85	7.307		
Entelodontidae	*Megachoerus latidens*	1829	34.2	7.307		
Entelodontidae	*Megachoerus latidens*	1829	35.2	7.307		
Anthracotheriidae	*Bothriodon advena*	306.89	36.985	4.602	1.076	5.484
Entelodontidae	*Archaeotherium mortoni*	134	38.8	3.713	0.742	5.642
Entelodontidae	*Brachyhyops uintensis*	46	41.96	2.815	0.853	5.989
Helohyidae	*Achaenodon robustus*	191	45.04	4.07		
Helohyidae	*Helohyus milleri*	21.55	46.605	2.313	1.163	5.702
Helohyidae	*Helohyus milleri*	21.55	47.98	2.313		
Helohyidae	*Helohyus milleri*	21.55	50.39	2.313		
Diacodexeidae	*Bunophorus grangeri*	9.17	52.05	1.854	0.756	5.903
Diacodexeidae	*Bunophorus grangeri*	9.17	52.58	1.854		
Diacodexeidae	*Bunophorus grangeri*	9.17	53.125	1.854		
Diacodexeidae	*Diacodexis ilicis*	1.33	54.155	1.124	1.11	5.849

Anthracotheriidae	*Arretotherium acridens*	191.77	18	4.074		
Anthracotheriidae	*Arretotherium acridens*	191.77	19	4.074		
Anthracotheriidae	*Arretotherium acridens*	191.77	21.25	4.074		
Anthracotheriidae	*Elomeryx* sp.	326.3	25.445	4.676		
Anthracotheriidae	*Kukusepasutanka schultzi*	344.59	28.82	4.742		
Anthracotheriidae	*Elomeryx armatus*	158.42	31	3.878	0.714	5.705
Anthracotheriidae	*Bothriodon americanus*	281.3	34.2	4.499		
Anthracotheriidae	*Bothriodon americanus*	281.3	35.2	4.499		
Anthracotheriidae	*Bothriodon advena*	306.89	36.985	4.602		
Anthracotheriidae	*Heptacodon pellionis*	75.72	38.8	3.203	0.97	5.672
Antilocapridae	*Tetrameryx shuleri*	64.65	0.125	3.074		
Antilocapridae	*Tetrameryx shuleri*	64.65	0.875	3.074		
Antilocapridae	*Tetrameryx* sp.	64.65	2	3.074		
Antilocapridae	*Tetrameryx* sp.	64.65	3.625	3.074		
Antilocapridae	*Hexameryx simpsoni*	30.65	5.25	2.534	0.697	5.764
Antilocapridae	*Hexameryx simpsoni*	30.65	7	2.534		
Antilocapridae	*Ilingoceros* sp.	49.85	8.25	2.874		
Antilocapridae	*Plioceros* sp.	17.76	9.5	2.2	0.838	5.695
Antilocapridae	*Plioceros* sp.	17.76	11.25	2.2		
Antilocapridae	*Ramoceros osborni*	22.13	13.05	2.329		
Antilocapridae	*Ramoceros ramosus*	22.13	14.3	2.329		
Antilocapridae	*Ramoceros ramosus*	22.13	15.5	2.329		
Antilocapridae	*Merriamoceros* sp.	14.91	16.75	2.103	0.42	5.752
Antilocapridae	*Merycodus sabulornis*	10.18	18	1.905	0.406	5.795
Diacodexeidae	*Tapochoerus egressus*	8.74	41.96	1.831		
Diacodexeidae	*Tapochoerus mcmillini*	4.29	45.04	1.523	0.676	6.265
Diacodexeidae	*Neodiacodexis emryi*	5.1	46.605	1.592		
Diacodexeidae	*Bunophorus pattersoni*	3.77	47.98	1.473	0.304	5.953
Diacodexeidae	*Bunophorus sinclairi*	8.92	50.39	1.841		
Diacodexeidae	*Bunophorus grangeri*	9.17	52.05	1.854		
Diacodexeidae	*Bunophorus grangeri*	9.17	52.58	1.854		
Diacodexeidae	*Bunophorus grangeri*	9.17	53.125	1.854		
Diacodexeidae	*Diacodexis ilicis*	1.33	54.155	1.124	1.11	5.849
Helohyidae	*Dyscritochoerus lapointensis*	29.05	38.8	2.499		
Helohyidae	*Achaenodon robustus*	191	45.04	4.07		
Helohyidae	*Helohyus milleri*	21.55	46.605	2.313	1.163	5.702
Helohyidae	*Helohyus milleri*	21.55	47.98	2.313		
Helohyidae	*Helohyus milleri*	21.55	50.39	2.313		
Homacodontidae	*Pentacemylus progressus*	5.79	38.8	1.646		

Homacodontidae	*Pentacemylus leotensis*	6.85	41.96	1.719		
Homacodontidae	*Auxontodon* sp.	5.63	45.04	1.634	0.116	6.264
Homacodontidae	*Homacodon* n. sp. A	3.25	46.605	1.417	0.564	6.012
Homacodontidae	*Homacodon* n. sp. A	3.25	47.98	1.417		
Homacodontidae	*Antiacodon vanvaleni*	2.1	50.39	1.266	0.464	6.255
Homacodontidae	*Antiacodon vanvaleni*	2.1	52.05	1.266		
Homacodontidae	*Hexacodus pelodes*	1.83	52.58	1.221	-0.037	5.63
Homacodontidae	*Hexacodus pelodes*	1.83	53.125	1.221		
Merycoidodontidae	*Merychyus* sp.	79.16	7	3.24		
Merycoidodontidae	*Merychyus major*	79.16	8.25	3.24		
Merycoidodontidae	*Merychyus novomexicanus*	119.76	9.5	3.607		
Merycoidodontidae	*Merychyus novomexicanus*	119.76	11.25	3.607		
Merycoidodontidae	*Merychyus novomexicanus*	119.76	13.05	3.607		
Merycoidodontidae	*Brachycrus siouense*	98	14.3	3.424	0.126	5.551
Merycoidodontidae	*Brachycrus laticeps*	248.61	15.5	4.358		
Merycoidodontidae	*Brachycrus laticeps*	248.61	16.75	4.358		
Merycoidodontidae	*Merycochoerus magnus*	325.53	18	4.673		
Merycoidodontidae	*Merycochoerus* sp.	252.51	19	4.375	0.229	5.345
Merycoidodontidae	*Merycochoerus* sp.	252.51	21.25	4.375		
Merycoidodontidae	*Merycochoerus pinensis*	252.51	25.445	4.375		
Merycoidodontidae	*Merycochoerus pinensis*	252.51	28.82	4.375		
Merycoidodontidae	*Eporeodon occidentalis*	63.01	31	3.054	0.966	5.773
Merycoidodontidae	*Merycoidodon culbertsoni/Oreodon macrorhinus*	46.84	32.85	2.828	0.296	5.799
Merycoidodontidae	*Merycoidodon culbertsoni/Oreodon macrorhinus*	46.84	34.2	2.828		
Merycoidodontidae	*Merycoidodon culbertsoni/Oreodon macrorhinus*	46.84	35.2	2.828		
Merycoidodontidae	*Merycoidodon culbertsoni/Oreodon macrorhinus*	46.84	36.985	2.828		
Merycoidodontidae	*Merycoidodon culbertsoni/Oreodon macrorhinus*	46.84	38.8	2.828		
Agriochoeridae	*Agriochoerus* sp.	43.31	25.445	2.771		
Agriochoeridae	*Agriochoerus gaudryi*	43.31	28.82	2.771		
Agriochoeridae	*Agriochoerus guyotianus*	23.84	31	2.374	0.6	5.929
Agriochoeridae	*Agriochoerus antiquus*	43.31	32.85	2.771		
Agriochoeridae	*Agriochoerus maximus*	43.31	34.2	2.771		
Agriochoeridae	*Agriochoerus maximus*	43.31	35.2	2.771		
Agriochoeridae	*Agriochoerus maximus*	43.31	36.985	2.771		
Agriochoeridae	*Agriochoerus maximus*	43.31	38.8	2.771		
Agriochoeridae	*Protoreodon pearcei*	27.53	41.96	2.464	0.48	6.082
Agriochoeridae	*Protoreodon pumilus*	15.54	45.04	2.125	0.581	6.129
Agriochoeridae	*Protoreodon* sp.	10.74	46.605	1.931	0.391	5.888

Dromomerycidae	*Pediomeryx hemphillensis*	145.19	5.25	3.791		
Dromomerycidae	*Pediomeryx hemphillensis*	145.19	6.125	3.791		
Dromomerycidae	*Pediomeryx(Yumaceras) figginsi*	233.43	7	4.287		
Dromomerycidae	*Pediomeryx(Yumaceras) hamiltoni*	233.43	8.25	4.287		
Dromomerycidae	*Cranioceras unicornis*	128.86	9.5	3.676	0.598	5.498
Dromomerycidae	*Cranioceras unicornis*	128.86	11.25	3.676		
Dromomerycidae	*Dromomeryx borealis*	205.03	13.05	4.146		
Dromomerycidae	*Dromomeryx borealis*	205.03	14.3	4.146		
Dromomerycidae	*Dromomeryx whitfordi*	132.81	15.5	3.705	0.462	5.486
Gelocidae	*Pseudoceras* sp.	6.34	7	1.685		
Gelocidae	*Pseudoceras* sp.	6.34	8.25	1.685		
Gelocidae	*Pseudoceras skinneri*	1.37	9.5	1.133	1.009	5.954
Gelocidae	*Pseudoceras* sp.	6.34	11.25	1.685		
Gelocidae	*Pseudoceras* sp.	6.34	13.05	1.685		
Leptochoeridae	*Leptochoerus* sp.	3.9	25.445	1.486		
Leptochoeridae	*Leptochoerus* sp.	3.9	28.82	1.486		
Leptochoeridae	*Leptochoerus* sp.	3.9	31	1.486		
Leptochoeridae	*Leptochoerus* sp.	3.9	32.85	1.486		
Leptochoeridae	*Leptochoerus* sp.	3.9	34.2	1.486		
Leptochoeridae	*Leptochoerus* sp.	3.9	35.2	1.486		
Leptochoeridae	*Stibarus yoderensis*	2.85	36.985	1.37	0.32	6.097
Leptochoeridae	*Ibarus ignotus*	2.24	41.96	1.287	0.206	6.574
Leptochoeridae	*"Diacodexis" woltonensis*	1.76	45.04	1.209	0.206	6.393
Leptochoeridae	*"Diacodexis" woltonensis*	1.76	46.605	1.209		
Leptochoeridae	*"Diacodexis" woltonensis*	1.76	47.98	1.209		
Leptochoeridae	*"Diacodexis" woltonensis*	1.76	50.39	1.209		
Leptochoeridae	*"Diacodexis" woltonensis*	1.76	52.05	1.209		
Moschidae	*Parablastomeryx gregoryi*	17.76	9.5	2.2		
Moschidae	*Longirostromeryx wellsi*	13.06	11.25	2.032	0.312	5.918
Moschidae	*Longirostromeryx wellsi*	13.06	13.05	2.032		
Moschidae	*Blastomeryx elegans*	11.62	14.3	1.971	-0.109	5.796
Moschidae	*Blastomeryx elegans*	11.62	15.5	1.971		
Moschidae	*Parablastomeryx* sp.	15.15	16.75	2.111		
Moschidae	*Parablastomeryx galushi*	15.15	18	2.111		
Moschidae	*Blastomeryx* sp.	7.39	19	1.753	0.68	5.715
Moschidae	*Blastomeryx elegans*	11.62	21.25	1.971		
Oromerycidae	*Eotylopus reedi*	23.57	34.2	2.367		
Oromerycidae	*Eotylopus reedi*	23.57	35.2	2.367		

Oromerycidae	*Montanatylopus matthewi*	79.16	36.985	3.24		
Oromerycidae	*Eotylopus reedi*	23.57	38.8	2.367	0.907	5.815
Oromerycidae	*Eotylopus reedi*	23.57	41.96	2.367		
Oromerycidae	*Protylopus petersoni*	5.13	45.04	1.595	1.007	6.197
Protoceratidae	*Kyptoceras amatorum*	300.35	5.25	4.576		
Protoceratidae	*Synthetoceras tricornatus*	211.19	8.25	4.177	0.371	5.836
Protoceratidae	*Synthetoceras tricornatus*	211.19	9.5	4.177		
Protoceratidae	*Synthetoceras tricornatus*	211.19	11.25	4.177		
Protoceratidae	*Lambdoceras trinitensis*	154.77	13.05	3.854	0.316	5.652
Protoceratidae	*Prosynthetoceras* sp.	51.86	14.3	2.904	0.863	5.571
Protoceratidae	*Lambdoceras siouxensis*	163	15.5	3.906		
Protoceratidae	*Lambdoceras hessei*	98	16.75	3.424	0.53	5.533
Protoceratidae	*Prosynthetoceras texanus*	49.31	18	2.866	0.661	5.6
Protoceratidae	*Prosynthetoceras texanus*	49.31	19	2.866		
Protoceratidae	*Syndyoceras cooki*	73.3	21.25	3.176		
Protoceratidae	*Protoceras* sp.	43.31	25.445	2.771	0.545	6.15
Protoceratidae	*Protoceras skinneri*	43.31	28.82	2.771		
Protoceratidae	*Protoceras celer*	43.31	31	2.771		
Protoceratidae	*Pseudoprotoceras longinaris*	12.23	34.2	1.997	0.926	6.132
Protoceratidae	*Poabromylus taylori*	31.58	35.2	2.554		
Protoceratidae	*Pseudoprotoceras semicinctus*	31.93	36.985	2.561		
Protoceratidae	*Heteromeryx dispar*	22.83	38.8	2.348	0.35	5.869
Protoceratidae	*Heteromeryx dispar*	22.83	41.96	2.348		
Protoceratidae	*Leptoreodon major*	9.9	45.04	1.891	0.746	6.164
Tayassuidae	*Mylohyus fossilis*	67.97	0.125	3.115		
Tayassuidae	*Mylohyus fossilis*	67.97	0.875	3.115		
Tayassuidae	*Platygonus pearcei*	83.68	2	3.287		
Tayassuidae	*Catagonus brachydontus*	105.33	3.625	3.489		
Tayassuidae	*Catagonus brachydontus*	105.33	5.25	3.489		
Tayassuidae	*Catagonus brachydontus*	105.33	6.125	3.489		
Tayassuidae	*Prosthennops serus*	64.09	7	3.067	0.52	5.427
Tayassuidae	*Prosthennops serus*	64.09	8.25	3.067		
Tayassuidae	*"Prosthennops" niobrarensis*	46.86	9.5	2.829	0.32	5.628
Tayassuidae	*Prosthennops serus*	64.09	11.25	3.067		
Tayassuidae	*Hesperhys* sp.	110.19	13.05	3.53		
Tayassuidae	*Hesperhys* sp.	110.19	14.3	3.53		
Tayassuidae	*Hesperhys vagrans*	115.18	15.5	3.57		
Tayassuidae	*Hesperhys vagrans*	115.18	16.75	3.57		
Tayassuidae	*Hesperhys pinensis*	105.33	18	3.489	-0.225	5.549
Tayassuidae	*Hesperhys pinensis*	105.33	19	3.489		
Tayassuidae	*Thinohyus lentus*	51.02	28.82	2.892	0.684	6.49

Tayassuidae	*Thinohyus lentus*	51.02	31	2.892		
Tayassuidae	*Thinohyus lentus*	51.02	32.85	2.892		
Entelodontidae	*Daeodon hollandi*	1519	18	6.964		
Entelodontidae	*Daeodon hollandi*	1519	19	6.964		
Entelodontidae	*Daeodon hollandi*	1519	21.25	6.964		
Entelodontidae	*Daeodon hollandi*	1519	25.445	6.964		
Entelodontidae	*Daeodon hollandi*	1519	28.82	6.964		
Entelodontidae	*Megachoerus latidens*	1829	31	7.307		
Entelodontidae	*Megachoerus latidens*	1829	32.85	7.307		
Entelodontidae	*Megachoerus latidens*	1829	34.2	7.307		
Entelodontidae	*Megachoerus latidens*	1829	35.2	7.307		
Entelodontidae	*Archaeotherium mortoni*	134	36.985	3.713	1.241	5.527
Entelodontidae	*Archaeotherium mortoni*	134	38.8	3.713		
Entelodontidae	*Brachyhyops uintensis*	46	41.96	2.815	0.853	5.989
Entelodontidae	*Brachyhyops uintensis*	46	45.04	2.815		
Leptomerycidae	*Pseudoparablastomeryx francescita*	3.82	13.05	1.478		
Leptomerycidae	*Pseudoparablastomeryx scotti*	4.78	14.3	1.566		
Leptomerycidae	*Pseudoparablastomeryx scotti*	4.78	15.5	1.566		
Leptomerycidae	*Pseudoparablastomeryx scotti*	4.78	16.75	1.566		
Leptomerycidae	*Leptomeryx* sp.	6.7	18	1.709		
Leptomerycidae	*Pronodens silberlingi*	13.06	19	2.032		
Leptomerycidae	*Pronodens silberlingi*	13.06	21.25	2.032		
Leptomerycidae	*Pronodens silberlingi*	13.06	25.445	2.032		
Leptomerycidae	*Pronodens silberlingi*	13.06	28.82	2.032		
Leptomerycidae	*Leptomeryx evansi*	3.99	31	1.494	0.898	6.096
Leptomerycidae	*Leptomeryx evansi*	3.99	32.85	1.494		
Leptomerycidae	*Leptomeryx mammifer*	11.63	34.2	1.972		
Leptomerycidae	*Leptomeryx mammifer*	11.63	35.2	1.972		
Leptomerycidae	*Leptomeryx mammifer*	11.63	36.985	1.972		
Leptomerycidae	*Leptomeryx yoderi*	6.39	38.8	1.688	0.601	5.997
Leptomerycidae	*Leptomeryx* sp.	6.7	41.96	1.709		
Camelidae	*Camelops hesternus*	1100	0.125	6.405		
Camelidae	*Gigantocamelus spatulus*	3674	0.875	8.754		
Camelidae	*Gigantocamelus spatulus*	3674	2	8.754		
Camelidae	*Gigantocamelus spatulus*	3674	3.625	8.754		
Camelidae	*Megacamelus merriami*	2162	5.25	7.63	0.548	5.298
Camelidae	*Megatylopus matthewi*	3005	6.125	8.31		
Camelidae	*Megatylopus gigas*	1486	7	6.924	0.672	5.061
Camelidae	*Megatylopus gigas*	1486	8.25	6.924		
Camelidae	*Megatylopus primaevus*	1400	9.5	6.818	-0.433	5.228

Camelidae	*Megatylopus* sp.	1400	11.25	6.818	-1.545	
Camelidae	*Megatylopus* sp.	1400	13.05	6.818		
Camelidae	*Aepycamelus robustus*	446	14.3	5.07	0.882	5.326
Camelidae	*Procamelus leptocolon*	500	15.5	5.222		
Camelidae	*Aepycamelus procerus*	488	16.75	5.189	-0.791	5.38
Camelidae	*Protolabis* sp.	176.06	18	3.985	0.832	5.438
Camelidae	*Protolabis* sp.	176.06	19	3.985		
Camelidae	*Stenomylus hitchcocki*	58.65	21.25	2.998	0.865	5.812
Camelidae	*Pseudolabis dakotensis*	50.57	25.445	2.885	-0.005	6.154
Camelidae	*Pseudolabis dakotensis*	50.57	28.82	2.885		
Camelidae	*Pseudolabis dakotensis*	50.57	31	2.885		
Camelidae	*Paratylopus labiatus*	34.8	32.85	2.619	0.396	5.828
Camelidae	*Poebrotherium* sp.	23.57	34.2	2.367	0.415	5.734
Camelidae	*Poebrotherium* sp.	23.57	35.2	2.367		
Camelidae	*Poebrotherium chadronense*	24.43	36.985	2.389		
Hypertragulidae	*Nanotragulus ordinatus*	4.26	19	1.52		
Hypertragulidae	*Nanotragulus ordinatus*	4.26	21.25	1.52		
Hypertragulidae	*Nanotragulus* sp.	2.08	25.445	1.262	0.679	6.481
Hypertragulidae	*Nanotragulus fontanus*	3.05	28.82	1.394		
Hypertragulidae	*Nanotragulus* sp.	2.08	31	1.262	0.407	6.216
Hypertragulidae	*Nanotragulus planiceps*	1.79	32.85	1.214	0	6.174
Hypertragulidae	*Hypertragulus calcaratus*	3.05	34.2	1.394		
Hypertragulidae	*Hypertragulus heikeni*	4.35	35.2	1.528		
Hypertragulidae	*Hypertragulus heikeni*	4.35	36.985	1.528		
Hypertragulidae	*Hypertragulus heikeni*	4.35	38.8	1.528		
Hypertragulidae	*Simimeryx minutus*	1.08	41.96	1.065	0.968	6.392

References

1. Smith FA, *et al.* (2010) The evolution of maximum body size of terrestrial mammals. *Science* 330:1216-1219.
2. Lewontin RC (1966) On the measurement of relative variability. *Syst. Zool.* 15(2):141-142.
3. Smith RJ (1984) Allometric scaling in comparative biology: problems of concept and method. *American Journal of Physiology* 246(2):R152-R160.
4. Van Valkenburgh B (1990) Skeletal and dental predictors of body mass in carnivores. *Body Size in Mammalian Paleobiology: Estimation and Biological Implications,* eds Damuth J & MacFadden BJ (Cambridge University Press, Cambridge), pp 182-205.
5. Silva M & Downing JA (1995) *CRC Handbook of Mammalian Body Masses* (CRC Press, Boca Raton).
6. Gingerich PD (2001) Rates of evolution on the time scale of the evolutionary process. *Genetica* 112-113:127-144.
7. Mattila TM & Bokma F (2008) Extant mammal body masses suggest punctuated equilibrium. *Proc. R. Soc. London Ser. B* 275:2195-2199.
8. Yablokov AV (1974) *Variability of Mammals* (Amerind Publishing, New Dehli).
9. Ruff CB, Trinkaus E, & Holliday TW (1997) Body mass and encephalization in Pleistocene Homo. *Nature* 387(6629):173-176.
10. Mead AJ (2000) Sexual dimorphism and paleoecology in *Teleoceras*, a North American Miocene rhinoceros. *Paleobiology* 26(4):689-706.
11. Gingerich PD (1993) Rates of evolution in Plio-Pleistocene mammals: six case studies. *Morphological Change in Quaternary Mammals of North America*, eds Martin RA & Barnosky AD (Cambridge University Press, Cambridge), pp 84-106.
12. Hamilton MJ, Davidson AD, Sibly RM, & Brown JH (2011) Universal scaling of production rates across mammalian lineages. *Proc. R. Soc. London Ser. B* 278(1705):560-566.
13. R Development Core Team (2009) *R: A Language and Environment for Statistical Computing v2.10.1* (R Foundation for Statistical Computing, Vienna).
14. Millien V (2006) Morphological evolution is accelerated among island mammals. *PLoS Biology* 4(10):1863-1868.
15. Hunt G (2007) The relative importance of directional change, random walks, and stasis in the evolution of fossil lineages. *Proc. Natl Acad. Sci. USA* 104(47):18404-18408.
16. Lister AM (1989) Rapid dwarfing of red deer on Jersey in the last interglacial. *Nature* 342(6249):539-542.
17. Roth VL (1992) Inferences from allometry and fossils: Dwarfing of elephants on islands. *Oxf. Surv. Evol. Biol.* 8:259-288.
18. Davies P & Lister AM (2001) *Palaeoloxodon cypriotes*, the dwarf elephant of Cyprus: size and scaling comparisons with *P. falconeri* (Sicily-Malta) and mainland *P. antiquus*. *The World of Elephants: Proceedings of the 1st International Congress, Rome 2001*, ed Cavarretta G (Ufficio Pubblicazioni, Rome), pp 479-480.
19. Lister A & Bahn PG (2007) *Mammoths: Giants of the Ice Age* (University of California Press, Berkeley, Calif.) Rev. Ed.
20. Christiansen P (2004) Body size in proboscideans, with notes on elephant metabolism. *Zool. J. Linn. Soc.* 140(4):523-549.

21. Benton MJ, *et al.* (2010) Dinosaurs and the island rule: The dwarfed dinosaurs from Hateg Island. *Palaeogeogr. Palaeoclimatol. Palaeoecol.* 293(3-4):438-454.
22. Quintana J, Koehler M, & Moya-Sola S (2011) *Nuralagus rex*, gen. et sp. nov., an endemic insular giant rabbit from the Neogene of Minorca (Balearic Islands, Spain). *J. Vert. Paleont.* 31(2):231-240.
23. Renaud S, Michaux J, Jaeger JJ, & Auffray JC (1996) Fourier analysis applied to Stephanomys (Rodentia, Muridae) molars: Nonprogressive evolutionary pattern in a gradual lineage. *Paleobiology* 22(2):255-265.
24. Anderson RP & Handley CO (2001) A new species of three-toed sloth (Mammalia: Xenarthra) from Panama, with a review of the genus *Bradypus*. *Proceedings of the Biological Society of Washington* 114(1):1-33.
25. Anderson RP & Handley CO (2002) Dwarfism in insular sloths: Biogeography, selection, and evolutionary rate. *Evolution* 56(5):1045-1058.
26. Bader RS (1955) Variability and evolutionary rate in the oreodonts. *Evolution* 9(2):119-140.
27. Janis CM (1990) Correlation of cranial and dental variables with body size in ungulates and macropodoids. *Body Size in Mammalian Paleobiology: Estimation and Biological Implications*, eds Damuth J & MacFadden BJ (Cambridge University Press, Cambridge), pp 255-299.
28. Berry RJ (1964) Evolution of island population of house mouse. *Evolution* 18(3):468-&.
29. Berry RJ, Jakobson ME, & Peters J (1978) The House mice of Faroe Islands: a study in microdifferentiation. *Journal of Zoology* 185(MAY):73-92.
30. Clyde WC & Gingerich PD (1994) Rates of evolution in the dentition of early Eocene *Cantius*: comparison of size and shape. *Paleobiology* 20(4):506-522.
31. Gingerich PD, Smith BH, & Rosenberg K (1982) Allometric scaling in the dentition of primates and prediction of body weight from tooth size in fossils. *Am. J. Phys. Anthropol.* 58(1):81-100.
32. Davis S (1977) Size variation of fox, *Vulpes vulpes* in palaearctic region today, and in Israel during late Quaternary. *Journal of Zoology* 182(JUL):343-351.
33. Forsten A (1990) Dental size trends in an equid sample from the Sandalja II cave of northwestern Yugoslavia. *Paläontologische Zeitschrift, Stuttgart* 64:153-160.
34. Goodwin HT (1993) Patterns of dental variation and evolution in prairie dogs, genus *Cynomys*. *Morphological Change in Quaternary Mammals of North America*, eds Martin RA & Barnosky AD (Cambridge University Press, Cambridge), pp 107-133.
35. Legendre S (1986) Analysis of mammalian communities from the late Eocene and Oligocene of southern France. *Palaeovertebrata* 16:191-212.
36. Guthrie RD (2003) Rapid body size decline in Alaskan Pleistocene horses before extinction. *Nature* 426(6963):169-171.
37. Scott KM (1990) Postcranial dimensions of ungulates as predictors of body mass. *Body Size in Mammalian Paleobiology: Estimation and Biological Implications*, eds Damuth J & MacFadden BJ (Cambridge University Press, Cambridge), pp 301-335.
38. Klein RG (1995) The Tor Hamar fauna. *Prehistoric Cultural Ecology and Evolution: Insights from Southern Jordan*, ed Henry DO (Plenum, New York), pp 405–416.
39. Klein RG & Scott K (1989) Glacial interglacial size variation in fossil spotted hyenas (*Crocuta crocuta*) from Britain. *Quat. Res.* 32(1):88-95.

40. Köhler M & Moyà-Solà S (2004) Reduction of brain and sense organs in the fossil insular bovid *Myotragus*. *Brain Behav. Evol.* 63(3):125-140.
41. Lich DK (1990) *Cosomys primus*: a case for stasis. *Paleobiology* 16(3):384-395.
42. Martin RA (1990) Estimating body mass and correlated variables in extinct mammals: travels in the fourth dimension. *Body Size in Mammalian Paleobiology: Estimation and Biological Implications*, eds Damuth J & MacFadden BJ (Cambridge University Press, Cambridge), pp 49-68.
43. Marshall LG (1973) The Lake Victoria Local Fauna. MSc. thesis, Vols. I + II MSc. thesis (Monash University, Melbourne, Australia).
44. Bartholomai A (1971) Morphology and variation of the cheek teeth in *Macropus giganteus* Shaw and *Macropus agilis* (Gould). *Memoirs of the Queensland Museum* 16:1-18.
45. Marshall LG & Hope JH (1973) A reevaluation of *Dasyurus bowlingi* Spencer and Kershaw 1910 (Marsupialia, Dasyuridae) from King Island, Bass Strait. *Proceedings of the Royal Society of Victoria* 85(2):225-236.
46. Gordon CL (2003) A first look at estimating body size in dentally conservative marsupials. *Journal of Mammalian Evolution* 10(1/2):1-21.
47. Martin RA (1986) Energy, ecology, and cotton rat evolution. *Paleobiology* 12(4):370-382.
48. McDonald JN (1981) *North American Bison: their Classification and Evolution* (University of California Press, Berkeley).
49. Millien V (2004) Relative effects of climate change, isolation and competition on body-size evolution in the Japanese field mouse, *Apodemus argenteus*. *J. Biogeogr.* 31(8):1267-1276.
50. Millien-Parra V (2000) Species differentiation among muroid rodents on the basis of their lower incisor size and shape: ecological and taxonomical implications. *Mammalia* 64(2):221-239.
51. Millien V & Damuth J (2004) Climate change and size evolution in an island rodent species: New perspectives on the island rule. *Evolution* 58(6):1353-1360.
52. Polly PD (2001) Paleontology and the comparative method: ancestral node reconstructions versus observed node values. *Am. Nat.* 157(6):596-609.
53. Prothero DR & Heaton TH (1996) Faunal stability during the Early Oligocene climatic crash. *Palaeogeogr. Palaeoclimatol. Palaeoecol.* 127(1-4):257-283.
54. Jones KE*, et al.* (2009) PanTHERIA: a species-level database of life history, ecology, and geography of extant and recently extinct mammals. *Ecology* 90(9):2648.
55. Smith FA (1992) Evolution of body size among woodrats from Baja California, Mexico. *Funct. Ecol.* 6(3):265-273.
56. Smith FA, Betancourt JL, & Brown JH (1995) Evolution of body size in the woodrat over the past 25,000 years of climate change. *Science* 270(5244):2012-2014.
57. Smith FA & Betancourt JL (1998) Response of bushy-tailed woodrats (*Neotoma cinerea*) to late Quaternary climatic change in the Colorado Plateau. *Quat. Res.* 50(1):1-11.
58. Smith FA & Betancourt JL (2003) The effect of Holocene temperature fluctuations on the evolution and ecology of *Neotoma* (woodrats) in Idaho and northwestern Utah. *Quat. Res.* 59(2):160-171.

59. Smith FA & Betancourt JL (2006) Predicting woodrat (*Neotoma*) responses to anthropogenic warming from studies of the palaeomidden record. *J. Biogeogr.* 33(12):2061-2076.
60. Szuma E (2003) Microevolutionary trends in the dentition of the Red fox (*Vulpes vulpes*). *Journal of Zoological Systematics and Evolutionary Research* 41(1):47-56.
61. Lister AM (2004) Ecological interactions of elephantids in Pleistocene Eurasia: *Palaeoloxodon* and *Mammuthus*. *Human Paleoecology in the Levantine Corridor*, eds Goren-Inbar N & Speth JD (Oxbow, Oxford), pp. 53-60.